

**University of South Bohemia**  
**Faculty of Science**

**Bachelor Thesis**

**Theoretical Study of Tautomeric Forms of Uracil and Their  
Interactions with  $Mg^{2+}$**

**Ingrid Romancová**

Supervisor: Mgr. Zdeněk Chval, Ph.D.

České Budějovice 2009

Romancová I., 2009: Theoretical Study of Tautomeric Forms of Uracil and Their Interactions with  $Mg^{2+}$ . Bc. Thesis, in English - 68 p., Faculty of Science, The University of South Bohemia, České Budějovice, Czech Republic.

Annotation:

This bachelor thesis is focused on theoretical study of uracil tautomers and their interactions with bare and hydrated  $Mg^{2+}$  cation in the gas phase. The main aim was to find the most stable complexes of  $Mg^{2+}$  ion with different uracil tautomers and compare their relative and interaction energies. A comparison with analogous  $Mg^{2+}$  complexes with thymine tautomers was also done and influence of the metal ion hydration on the relative stability of the tautomers was evaluated.

Prohlašuji, že svoji bakalářskou práci jsem vypracovala samostatně pouze s použitím pramenů a literatury uvedených v seznamu citované literatury.

Prohlašuji, že v souladu s § 47b zákona č. 111/1998 Sb. v platném znění souhlasím se zveřejněním své bakalářské práce, a to v nezkrácené podobě – v úpravě vzniklé vypuštěním vyznačených částí archivovaných Přírodovědeckou fakultou - elektronickou cestou ve veřejně přístupné části databáze STAG provozované Jihočeskou univerzitou v Českých Budějovicích na jejích internetových stránkách.

V Českých Budějovicích 30. dubna 2009

Podpis studenta

## **Aknowledgments**

I thank a number of people for helpful comments on my bachelor thesis. I thank my supervisor Mgr. Zdeněk Chval, Ph.D. for helpful advice and discussions, for the correction of this thesis. I would like to thank Mgr. Martin Kabeláč, Ph.D. for his useful lectures about Computational Chemistry and RNDr. Milan Předota, Ph.D. for his simulation course.

# Content

1 Introduction.....	1
1.1 Magnesium [Mg].....	1
1.1.1 History of Magnesium.....	1
1.1.2 General Chemical Properties.....	1
1.2 Interactions between Hydrated Magnesium Ion and Nucleic Acids.....	3
1.3 Biological Role of Magnesium.....	4
1.4 Nucleic acids.....	5
1.4.1 Chemical structure.....	5
1.5 Interaction between Magnesium ion and Nucleic Acid.....	13
1.6 Catalytic Nucleic Acids.....	14
1.7 The Interactions between Metal Ions and Catalytic Nucleic Acids.....	17
1.7.1 The Significant Role of Metal Ions in Catalytic Nucleic Acid Reactions.....	18
1.8 Tautomerization Process.....	20
1.8.1 Nucleic Acid Hydration.....	20
1.8.2 Tautomerism of Nucleobases.....	21
1.8.3 Tautomerism of Uracil.....	23
1.8.4 The Proton-Transfer Process in a Microhydrated Environment.....	24
1.8.5 Interaction of Uracil with metal ions with Respect to the Tautomerization Process.....	24
1.9 The Introduction to Quantum Chemistry and Computational Chemistry.....	26
1.9.1 LCAO - a linear combination of atomic orbitals.....	26
1.9.2 The variational method.....	26
1.9.3 The Born-Oppenheimer Approximation.....	27
1.9.4 Slater Determinant.....	29
1.9.5 Ab Initio Calculations.....	30
1.9.5.1 Hartree-Fock Theory (SCF).....	30
1.9.5.2 Density Functional Theory (DFT).....	31
2 Methods .....	33
3 Results.....	34
3.1 Tautomerism of uracil.....	34
3.2 Mg <sup>2+</sup> Binding to All Tautomers of Uracil.....	37
3.3 The Comparison of Mg <sup>2+</sup> binding to the most stable Tautomers of Thymine and Uracil.....	51
3.4 Binding of Hydrated Magnesium Ion to Uracil Tautomers.....	59
4 Conclusions.....	63
References.....	64
Appendices.....	68

# 1 Introduction

## 1.1 Magnesium [Mg]

### 1.1.1 *History of Magnesium*

Magnesium compounds have been used since ancient times. Steatite (also known as soapstone, lard stone, talc, soaprock ...) has been found in Thessally called Magnesia. The name 'Magnesium' is originated from this region. The metal itself was first isolated by british chemist Sir Humphry Davy in 1808 (together with calcium, barium and strontium). He used electrolysis designed according to J. J. Berzelius and M.M. Pontin. The positive electrode (the anode) was platinum board, and the negative electrode (the cathode) was platinum wire immersed in the mercury. Davy was trying to isolate magnesium when he prepared magnesium amalgam. He distilled off all its mercury and obtained magnesium.<sup>1</sup>

### 1.1.2 *General Chemical Properties*

Magnesium is a chemical element with the atomic number 12. It belongs to alkaline-earth metals, it lies in the group IIA, the 3<sup>rd</sup> period. Magnesium is a silvery white metal. Its basic chemical and physical properties are shown in Tables 1 and 2.

In rocks magnesium is found in insoluble carbonate, sulphate and silicate compounds. Magnesium can be found in over 60 minerals. Magnesian limestone in Italy is called dolomite,  $\text{MgCa}(\text{CO}_3)_2$ . Magnesite is magnesium carbonate,  $\text{MgCO}_3$ . Epsomite is hydrous magnesium sulphate,  $\text{MgSO}_4 \cdot 7\text{H}_2\text{O}$ . Carnallite is a hydrated potassium magnesium chloride,  $\text{K}_2\text{MgCl}_4 \cdot 6\text{H}_2\text{O}$ . Langbeinite is a potassium magnesium sulphate,  $\text{K}_2\text{Mg}_2(\text{SO}_4)_3$ . Other minerals are olivine (magnesium iron silicate,  $(\text{Mg,Fe})_2\text{SiO}_4$ ), talc (hydrated magnesium silicate,  $\text{Mg}_3\text{Si}_4\text{O}_{10}(\text{OH})_2$ ), asbestos (chrysotile,  $\text{Mg}_3\text{Si}_2\text{O}_5(\text{OH})_4$ ), spinel (semiprecious stone,  $\text{MgAl}_2\text{O}_4$ ).<sup>1</sup>

*Table 1: General Chemical Properties of Magnesium*

<b>Name</b>	Magnesium
<b>Symbol</b>	Mg
<b>Atomic number</b>	12
<b>Group in periodic table</b>	IIA
<b>Group name</b>	Alkaline-earth metal
<b>Period in periodic table</b>	3
<b>Block in periodic table</b>	s-block
<b>Appearance</b>	silvery white metal
<b>Atomic weight</b>	24.3050
<b>Electron configuration</b>	[Ne]3s <sup>2</sup>
<b>Standard state at room temp</b>	solid
<b>Electron per shell</b>	2, 8, 2
<b>Ionization energy [kJ mol<sup>-1</sup>]</b>	737.5
<b>Metal radius [pm]</b>	160
<b>Ionic radius [pm]</b>	72 (4-coordinate)
<b>Number of naturally occurring isotopes</b>	3
<b>E°/V for M<sup>2+</sup>(aq) + 2e → M(s)</b>	2.37
<b>Oxidation states</b>	2

*Table 2: Physical Properties of Magnesium*

<b>Melting point [°C]</b>	649
<b>Boiling point [°C]</b>	1105
<b>Density(20°C) [g cm<sup>-3</sup>]</b>	1.738
<b>Heat of fusion [kJ mol<sup>-1</sup>]</b>	8.9
<b>Heat of vaporization [kJ mol<sup>-1</sup>]</b>	127.4
<b>Electrical resistivity(20°C) [μΩ cm]</b>	4.46

## 1.2 Interactions between Hydrated Magnesium Ion and Nucleic Acids

Two basic interactions were found between hydrated magnesium ion and nucleic acids:

1. direct coordination interactions between electronegative elements of nucleic acids and magnesium ion
2. hydrogen bonds interactions

The presence of magnesium ion is very important for nucleic acids structure.  $Mg^{2+}$  has an influence on geometry and crystal packing of the double helix. Bivalent cations have effect on ligand binding and folding of nucleic acids.

The bivalent magnesium ion has higher polarization activity than monovalent cations as a result of its high charge to radius ratio.

In solution the magnesium ion forms hexacoordinated structures of the octahedral shape. All six coordination positions can be occupied by water molecules (hexahydrated ions). When the magnesium ion comes in a contact with a biomolecule one or more water ligands can be exchanged for negatively charged groups of the biomolecule. Magnesium strongly prefers coordination to the groups with a negatively charged oxygen (aspartate and glutamate groups in proteins, phosphate group in nucleic acids). Coordination to N and S is much less common. Magnesium ion keeps usually its octahedral arrangement of the ligands but there is some evidence of the lowering of the coordination number especially in the presence of the hydroxo group.<sup>2</sup>

In our study we have considered hexacoordinated magnesium ion studying the following systems: 1) the hexahydrated magnesium ion and uracil in the second coordination shell ( $Mg^{2+}$

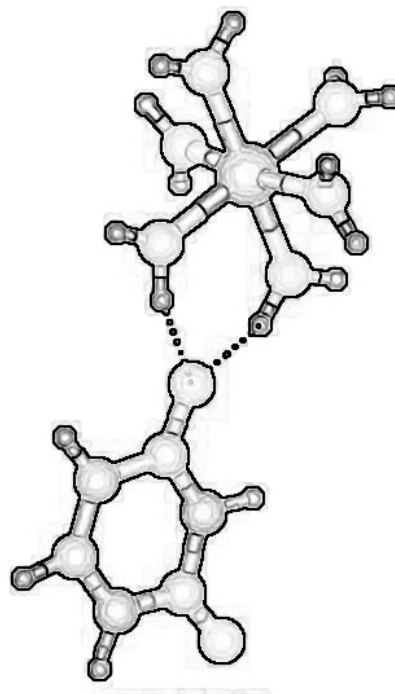


**Fig. 1** Hexahydrated magnesium ion and uracil

+6W+U) (see Figure 1);

2) the pentahydrated magnesium ion with uracil in the first coordination shell ( $Mg^{2+} + 5W + U$ );

3) the tetrahydrated magnesium ion with uracil and phosphate ion in the first coordination shell ( $Mg^{2+} + 4W + U + P$ ).<sup>3</sup>

### 1.3 Biological Role of Magnesium

Magnesium occurs as the  $Mg^{2+}$  ion in biological systems.  $Mg^{2+}$  dominates in the cytoplasm, rarely it does not create complexes.

The biologically active ATP is actually MgATP chelate. Glutamine synthetase has two metal-binding sites. The first site has high affinity and involves the catalytic cofactor, the second one has low affinity and underlies binding of the MgATP chelate. Divalent  $Mg^{2+}$  ions form octahedral structures with coordination to carboxylate residues. The  $Mg^{2+}$  ion has an important role during the formation of glutamine from glutamate and ammonia.

Chlorophyll is a key part of the light-harvesting complex in plants. Chlorophyll is a chlorin pigment and magnesium ion is located at the center of chlorine. The divalent cation is required for a synthesis of chlorophyll. The  $Mg^{2+}$  ion is able to adopt the octahedral geometry and stabilizes the structure without energy loss of fluorescence.

The  $Mg^{2+}$  ion is an active metal ion in the regulation of RuBisCo enzyme activity. A carbamate ion is formed as a result of the pH change and the presence of magnesium ions. The RuBisCo enzyme takes a share in removing carbon dioxide molecule from atmosphere. If we illuminate the chloroplast, the proton gradient is formed across the thylakoid membrane and the pH value of the stroma increases. Magnesium ions move out of the thylakoids and their concentration rises in the stroma. The optimal pH value for RuBisCo activity is greater than 9.0.

Magnesium participates by two basic ways of in enzymatic reactions.

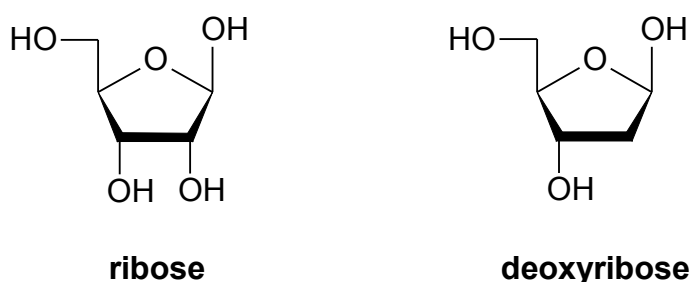
1. Enzyme binds the magnesium-substrate complex.
2. The  $Mg^{2+}$  ion binds directly to the enzyme.

The interactions between magnesium ion and enzymes (or proteins) are usually weak or moderate with  $K_a \leq 10^5 M^{-1}$ . Citric acid cycle, glycolytic cycle and other metabolic cycles depends on magnesium-activated enzymes. Many enzymes require at least two metal-binding sites. The first one is an allosteric site (accountable either for structure or binding) and the second one has a catalytic role. Lewis acidity of  $Mg^{2+}$  provides a large number of hydrolyses and condensation reactions (commonly phosphate ester hydrolysis and phosphoryl transfer).<sup>4</sup>

## 1.4 Nucleic acids

### 1.4.1 Chemical structure

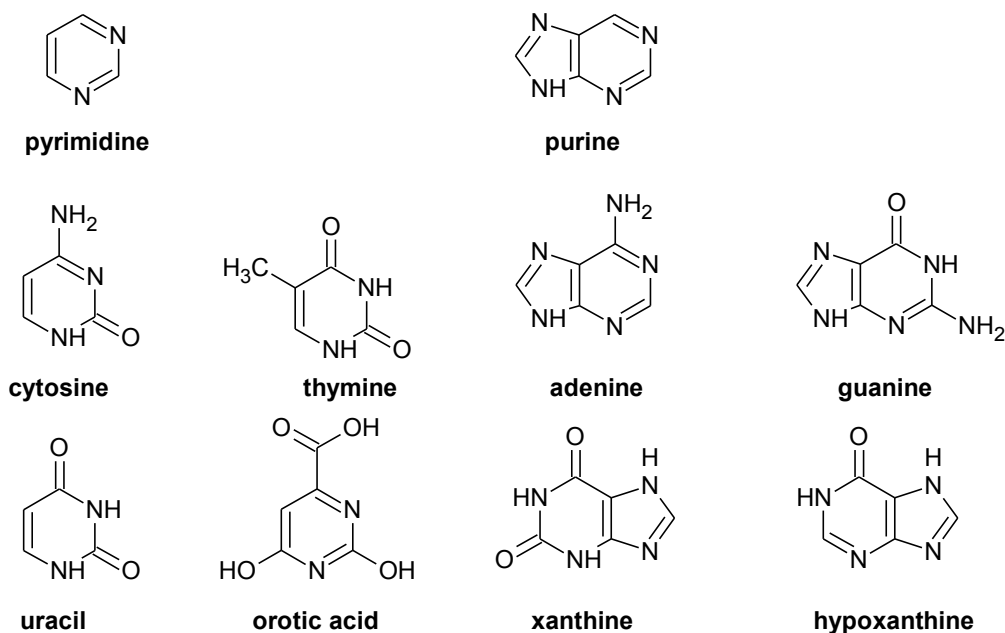
Nucleic acids are biological macromolecules that are elements of heredity and genetic information transfer. The principal components of their chain are nucleotides that consist of three other components: a nitrogenous heterocyclic base, which is a pyrimidine or a purine, a five-carbon sugar, which is a ribose or a deoxyribose, and an anion after the third dissociation of a phosphoric acid,  $PO_4^{3-}$ , the phosphate anion. There are two basic kinds of nucleic acids: deoxyribonucleic acids (DNA) and ribonucleic acid (RNA). The pentose sugar in DNA is 2-deoxy- $\beta$ -D-ribose, in RNA it is  $\beta$ -D-ribose. The difference between ribose and deoxyribose is in the presence of hydroxyl group on the C2 carbon (see Figure 2).



**Fig. 2** Schematic drawings of two basic kinds of pentose sugar - ribose and deoxyribose.

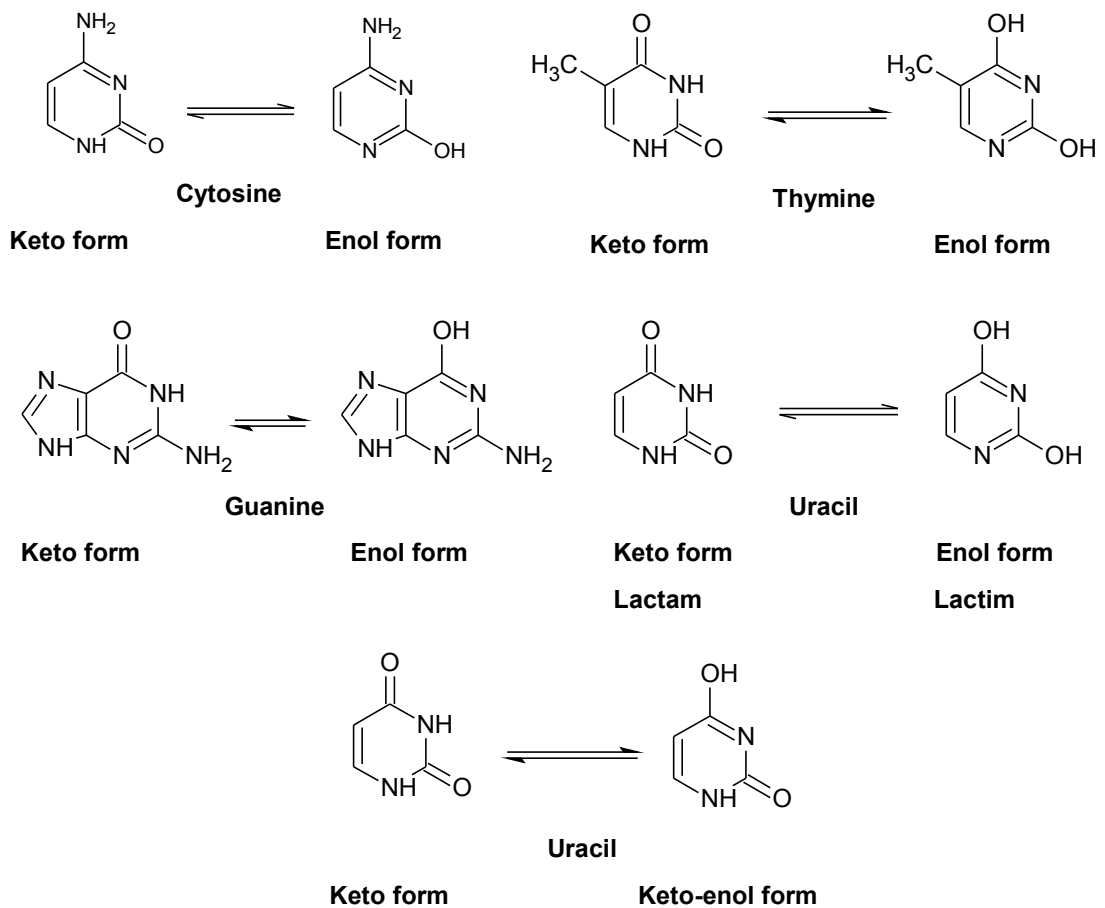
The nitrogenous heterocyclic bases are derivatives of either pyrimidine or purine. Pyrimidines have a six-membered nitrogen-containing ring. The pyrimidine bases are uracil (2,4-dioxy pyrimidine), cytosine (2-oxy-4-amino pyrimidine), thymine (2,4-

dioxy-5-methyl pyrimidine) and orotic acid (2,4-dioxy-6-carboxy pyrimidine). Purines consist of the two six- and five-membered nitrogen-containing rings (pyrimidine and five-membered imidazol ring), fused together. The purine bases are adenine (6-amino purine), guanine (2-amino-6-oxy purine) and xanthine (2,6-dioxy purine). Cytosine, thymine, guanine and adenine are typically found in DNA, while thymine is substituted by uracil in RNA. All these bases are planar aromatic systems (see Figure 3).



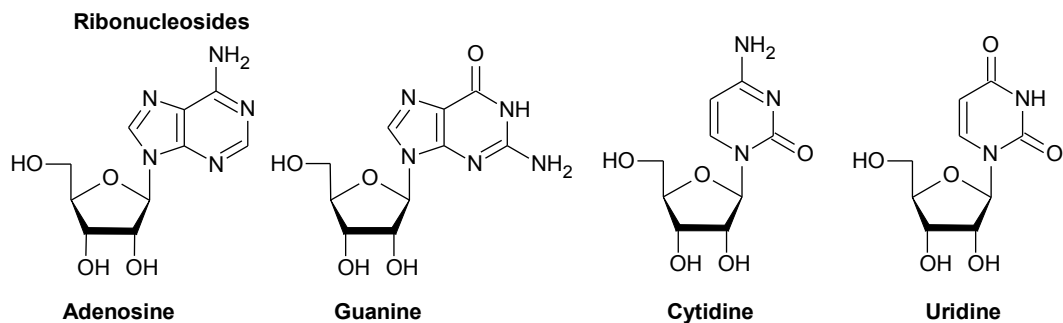
**Fig. 3** Schematic drawings of the nitrogenous heterocyclic bases.

These derivatives of purine and pyrimidine undergo keto-enol tautomeric shifts as a result of their aromatic ring and electronegative OH,  $\text{NH}_2$  and NH groups. In the case of uracil it undergoes amide-imidic acid tautomeric shift. The keto tautomer is called the lactam structure, while enol form is referred to the lactim structure (see Figure 4). However, the keto-enol forms of uracil occur in following study, too.



**Fig. 4** Schematic drawings of keto and enol forms purine and pyrimidine derivatives.

If a nitrogenous base joins to a sugar, it calls into existence of a nucleosid. These two compounds are joined via glycosidic bond. The sugar and the nitrogenous base can rotate around this bond and form synclinal or anticlinal conformation. In case of nucleosides and nucleotides only  $\beta$ -configuration is available. The nucleosides found in nucleic acids are cytidine, uridine, thymidine, adenosine and guanine (see Figure 5).



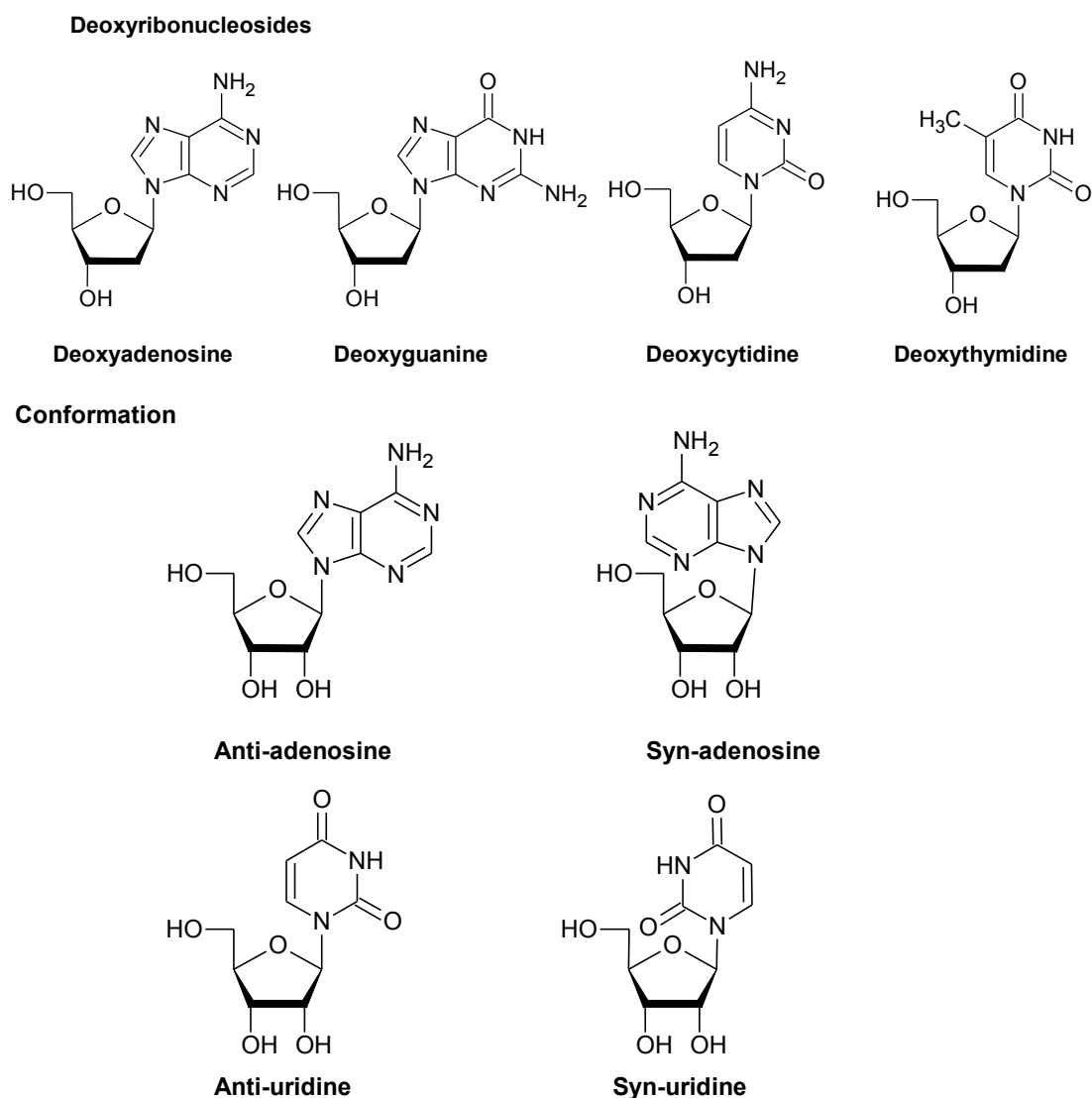


**Fig. 5** Schematic drawings of some ribonucleosides, deoxyribonucleosides and anticlinal versus synclinal conformation.

A nucleotide consists of one nucleoside and one phosphate group. In most cases we suppose that the phosphoric acid reacts by esterification with OH group at C-5' atom of pentose ring, but bond at C-2' and C-3' are available, too. In case of deoxyribose the hydroxyl group at the C2 position is reduced. Nucleoside bonded to a phosphate forms nucleoside monophosphate. It is customary to denote these monophosphates by three-letters abbreviations. Uridine-5'- monophosphate is called UMP, adenosine-5'- monophosphate is called AMP, etc. If other phosphates are added through the phosphoric anhydride linkages to the phosphoryl group of nucleotide, then the diphosphates or triphosphates are formed, in sequence. Adenosine-5'-diphosphate is referred as ADP, adenosine-5'-triphosphate is ATP. The phosphoric anhydride bonds

are primary source of chemical energy, for instance UTP play important role for biosynthesis complex carbohydrates and polysaccharides (see Figure 6).

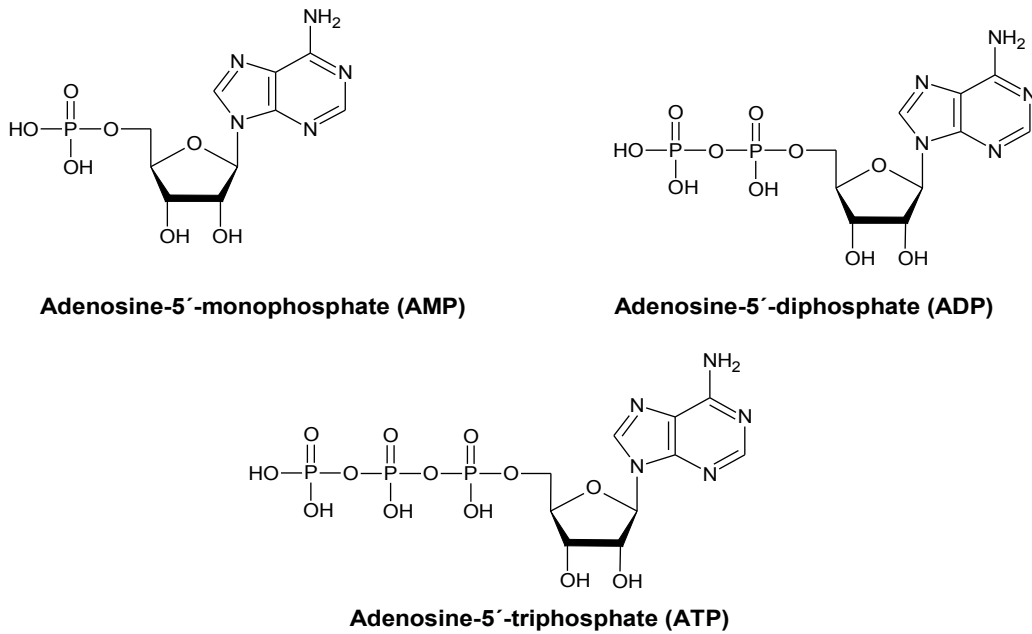


**Fig. 6** Formation of AMP,ADP, ATP via phosphoric anhydride linkages.

Nucleic acids are macromolecules whose chain is formed by joining mononucleotides together by phosphodiester bridges. Ribonucleic acid (RNA) contains ribose ring, deoxyribonucleotide polymers (DNA) consist of deoxyribose ring (see Figure 7).

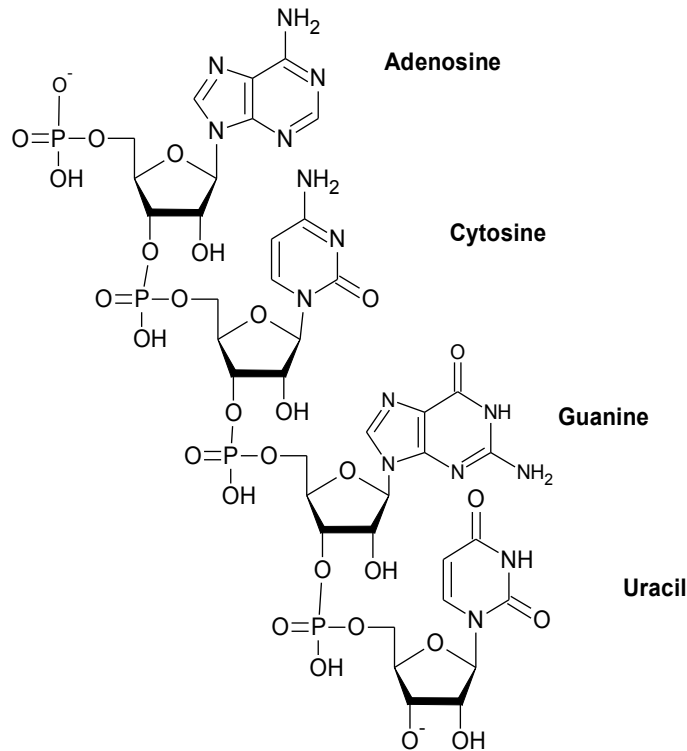


**Fig. 7** Polynucleotide chain of RNA - ApCpGpU

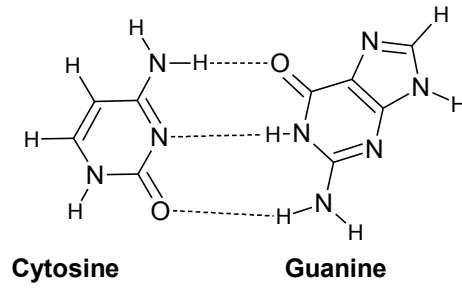
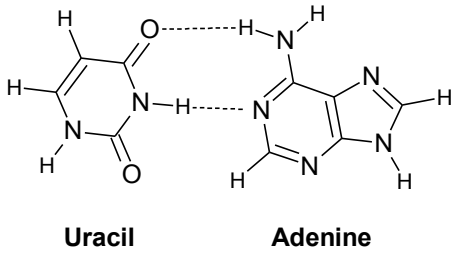
In DNA two nucleotide strands wind around each other to form a double helix. The DNA double helix is stabilized by hydrogen bonds between nitrogenous bases of each strand - base pairing and by stacking interactions between the base pairs. Hydrophilic and hydrophobic interactions are also important for the structure and stability of DNA. Charged and highly polar phosphate-deoxyribose chain is exposed to the solvent while less polar nitrogenous bases are headed to the inside of the helix. This arrangement protects the bases from reactive species that may occur in solution lowering thus probability of mutation.

In the standard base pairing pyrimidine bases bind always only to purine bases. It ensures that diameter of the helix is not sequence dependent. There are two types of base pairs differing in number of hydrogen bonds that stabilize the base pair. Base pairing is very specific, if adenine is in one strand, thymine must be in other. This type of base pair is stabilized by two hydrogen bonds. The second type of base pair is between cytosine and guanine forming three hydrogen bonds.

The size of DNA is usually expressed by the number of base-pairs. One thousand base-pairs can be expressed as 1 Kb or 1 kpb, one million base-pairs as 1 Mb or 1 mbp. The standard base pairing found in the native DNA is often called Watson-Crick base pairing. The isolated bases contain many functional groups that may serve as H-bond donors or acceptors therefore Watson-Crick binding pattern is not the unique one that is possible. As an example we can show Hoogsteen base-pairs (see Figure 8). They can be found e. g. in the three- and four-stranded DNA. Other types of nonstandard base-pairs can be found in RNA molecules.

In Figure 7 a part of a polynucleic chain of RNA is shown. If we substitute hydroxyl groups at C2 carbon of pentose ring by hydrogen atom, we obtain a polynucleic chain of DNA. Primary structure of DNA is represented by the nucleotide sequences written from the left (5'-end) to the right (3'-end). The properties of DNA depend on sequence of nitrogenous bases that gives to DNA its uniqueness. The strands can be linear or circular, double strand may have some loops (hairpin) or bulges (see Figure 9)

**Watson-Crick base pairing**



**Hoogsteen base pairing**

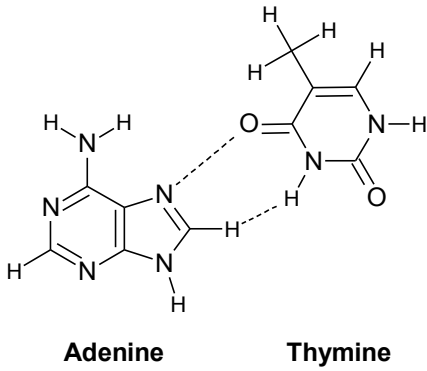


*Fig. 8 The Watson-Crick and Hoogsteen base pairs.*

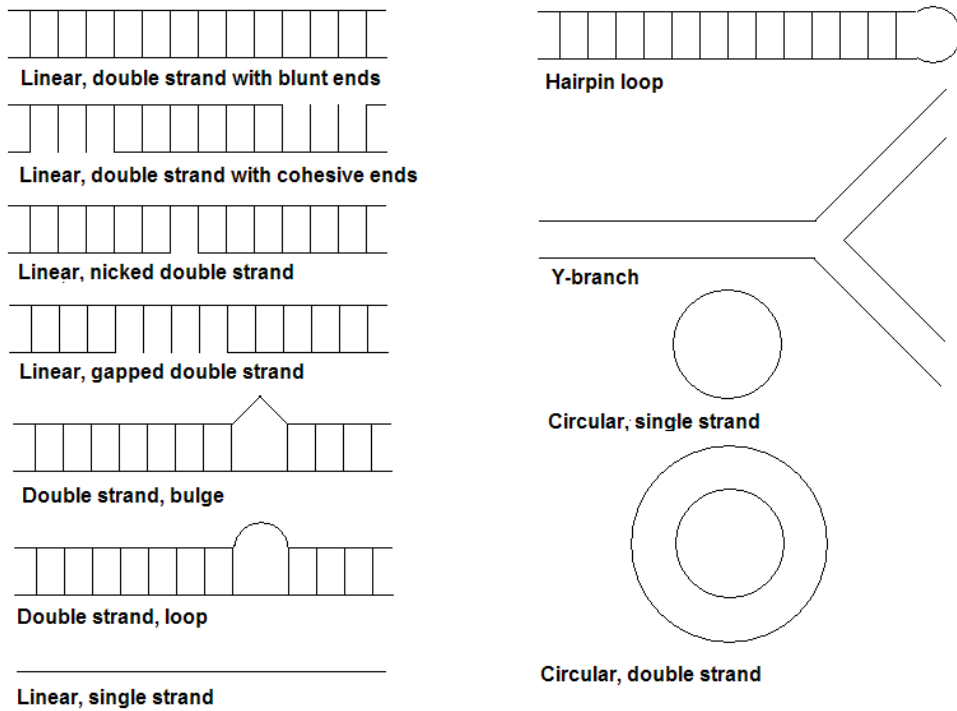


*Fig. 9 The types of DNA strands.*

Every DNA chain can be characterized by structural parameters. The space between two phosphodiester backbones is called a groove. There are two types of grooves - major and minor which differ by a width and a depth. Antisynclinal and synclinal orientation of a nitrogenous base joined to a sugar unit is the other structural parameter. Two DNA strands can form right-handed or left-handed helix. Puckering of the sugar is called endo, if the orientation of sugar directs from the plane to the base, or it is called exo, if the orientation is reversed. The number of bps determines bases residues per turn. Axial rise is distance between bases in direction of the axis. Base pair tilt, rotation per residue, base pair roll, propeller twist are the other structural parameters.

DNA double helix can form three basic conformation: A-, B- and Z- DNA (see Figure 10). The B- DNA can be separated into four subgroups - B, alt B, C and D (see Table 3). The right handed, anti-parallel B-form double helix represents the most significant biological conformation.

**Table 3: DNA polymorphism - secondary structures**

DNA form	A-form	B-form				Z-form	
		B	alt B	C	D	Z I	Z II
Helix sense	Right-handed	Right-handed	Right-handed	Right-handed	Right-handed	Left-handed	Left-handed
Puckering of the pentose	C <sub>3</sub> 'endo	C <sub>2</sub> 'endo	C <sub>2</sub> 'endo	C <sub>2</sub> 'endo (T) C <sub>3</sub> 'endo (A)	C <sub>2</sub> 'endo	C <sub>3</sub> 'endo	C <sub>3</sub> 'endo (G) C <sub>2</sub> 'endo (C)
Glycosidic bond	Anticlinal <sub>1</sub>	Anticlinal	Anticlinal	Anticlinal	Anticlinal	Anticlinal(C) Synclinal(G)	Anticlinal(C) Synclinal(G)
Residues per turn	11	10	10	9.3	8	12	12
Axial rise	2.6	3.4	3.4	3.3	3.0	3.2	3.3

The packing and conformation of secondary and tertiary structure of DNA are influenced by many interactions, that can exist between the different parts of DNA or between the DNA and the surrounding molecules. These interactions take place at the most rate:

1. Planar interactions between bases.
2. Vertical interactions.
3. Interactions with the surroundings.

Planar interactions are the result of H-bonds between the base pairs. These bonds are important for a base pairing and they help to form the secondary structure. Vertical interactions are stabilized by London dispersion interactions and are usually called the stacked interactions. Study of interactions with surroundings is the main aim of our study. Surroundings could be represented by monovalent or divalent cations, water, etc. The environment plays an important role in proton transfer and tautomerism of nucleic acid bases. Figure 9 represents conformational forms of DNA from the Nucleic Acid Database. The DNA conformation depends strongly on the concentration of ions.<sup>5-6</sup>

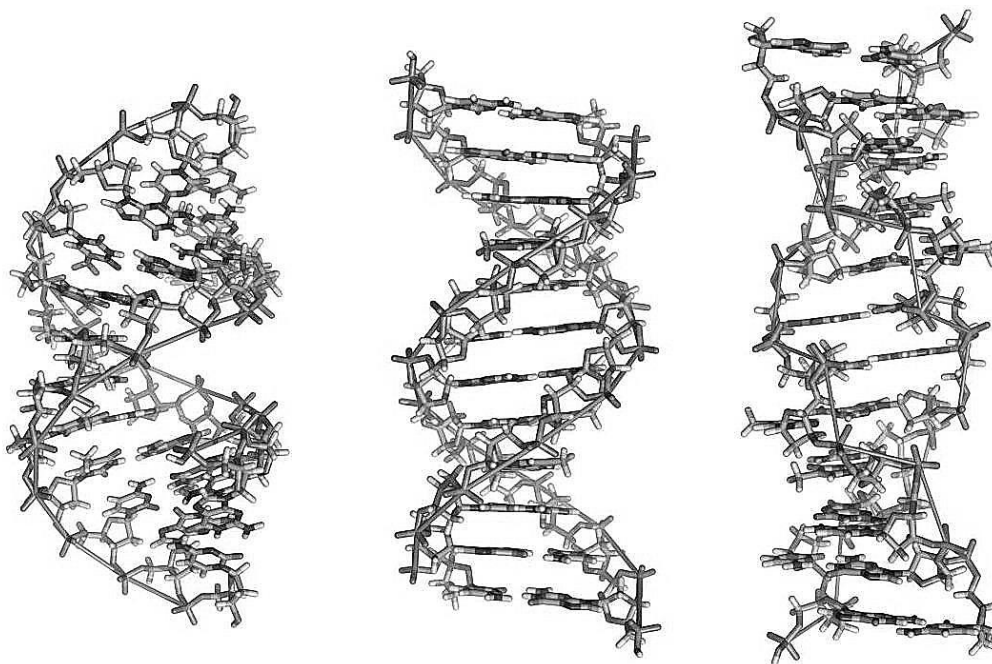


*Fig. 10* Nucleic acids structures represents three different types of DNA forms: A-form, B-form and Z-form in this order.

### 1.5 Interaction between Magnesium ion and Nucleic Acid

Magnesium divalent cation has several important properties that granted the cation to interact with nucleic acids.  $Mg^{2+}$  is a positively charged cation with small ionic radius (see Table 1). Its closed shell electronic structure is responsible for the fact that its interactions occur mainly through electrostatic forces. The electrostatic interaction

depends on the ion radius. Higher charge density causes stronger electrostatic interaction. Many studies show that  $Mg^{2+}$  plays an important role in the packing and conformation of secondary and tertiary structure of nucleic acids.

Nucleic acids create a strong electrostatic field and the negative charge of the phosphate groups causes a strong repulsion between the nucleotides. Cations compensate this negative charge. Water environment, typical surroundings of biological molecules - is an important for the stability of nucleic acids since electrostatic forces are suppressed in water due to its high value of dielectric constant.  $Mg^{2+}$  ion forms complexes with water molecules. When we submerge a cation into water, it will tend to be surrounded by anions, in this case the negatively charged phosphate groups will interact with magnesium cation minimizing their mutual charge repulsion.

RNA may form various tertiary motifs which may differ substantially in the charged density. In places with the high charged density of RNA there are located more cations than in place with smaller charge density.  $Mg^{2+}$  ions influence also ligand-DNA interactions. The position of ions near DNA may alter structural parameters of the double helix, minor groove size.

Nucleic acids folding is sensitive to  $Mg^{2+}$  concentrations.  $Mg^{2+}$  ion may induces tautomerism of nucleobases which may lead to mismatches in the base pairing and trigger spontaneous mutations. <sup>3,7-12</sup>

Metal ions help in proton-transfer reaction. The keto form tautomerize to its enol form due to phenomenon called water assisted proton transfer. Then the cation helps stabilize the rare tautomers. It may cause mutagenicity.

## **1.6 Catalytic Nucleic Acids**

In 80's some RNA molecules have been identified as RNA enzymes and they were called catalytic RNA, ribozymes. This was a very surprising discovery since up to this time only proteins had been thought to offer sufficient variability of functional groups to work as enzyme. As "normal" enzymes ribozymes enhance the reaction rate and they are substrate specific. Ribozymes catalyze peptidyl transferase reaction, transesterification or hydrolysis of phosphodiester bonds. In the following paragraphs

we will target only on the ribozymes.

Naturally occurring catalytic RNAs include the hammerhead, hairpin, glmS, hepatitis delta virus, Varkud satellite ribozymes, group I and group II introns and RNA subunit of RNase P (see Figure 11). Ribozymes could be distributed into two classes:

1. Class A - activates functional group 2'-OH for a nucleophilic attack on the phosphorus to cleave P-5'-O phosphodiester bond and products 2',3'- cyclic phosphate and 5'-OH termini. The length of ribozymes is smaller than 200 bases. This class included the hammerhead, hairpin, hepatitis delta virus, Varkud Satellite ribozymes.

2. Class B - uses an external nucleophile to attack adjacent scissile phosphodiester and products 3'-OH and 5'-phosphate termini. It includes RNase P, the group I and II intron ribozymes. These ribozymes are larger than 400 bases.<sup>13</sup>

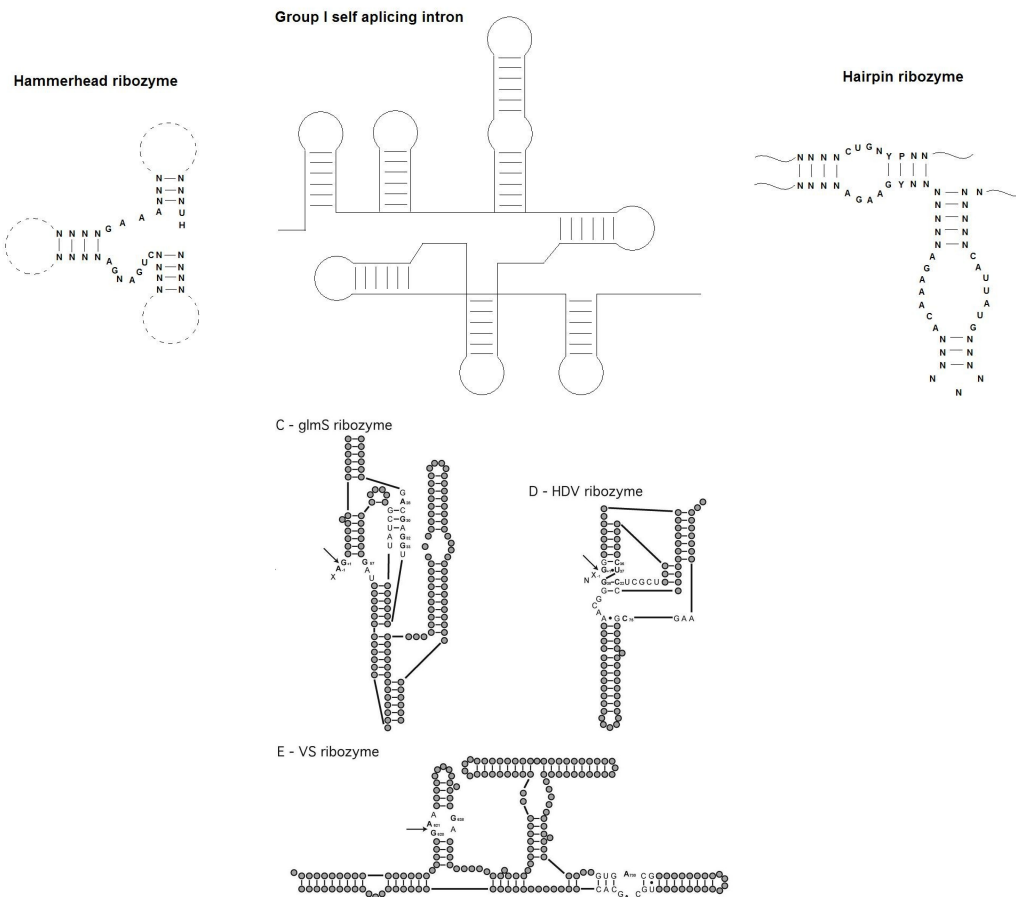


**Fig. 11** Naturally occurring catalytic RNAs. The last three figures were downloaded from <http://pubs.acs.org/action/showImage?doi=10.1021%2Far800050c&iName=master.img-001.jpg&type=master>

The simplest and the most studied catalytic RNA is the hammerhead ribozyme.

Hammerhead ribozymes are small self-cleaving RNAs found in viroids and satellite RNAs associated with plant RNA viruses. They were first discovered in 1986 in plant viroids. Hammerhead ribozyme consists of two strands, one strand catalyzes the cleavage of the other strand. The self-cleavage reaction includes 13 invariant core nucleotides that do not take part in Watson-Crick base-pairs. The core region consists of three stems - Stem I, Stem II and Stem III. The full-length hammerhead ribozyme contains special sequence elements in stems I and II that enable stabilization of the tertiary interactions stabilizing the active structure of the ribozyme that involves loop-bulge interactions between the stems I and stem II.<sup>14</sup>

The cleavage reaction is subjected to phosphodiester isomerization. The reaction is initiated by activation of 2' - hydroxyl group, which attacks the phosphorus atom and the cleavage proceeds by S<sub>N</sub>2 mechanism via a transition state with the "in-line" conformation of the attacking nucleophile and the leaving group. The role of divalent metal ions in hammerhead ribozyme catalysis has been a subject of a long term debate. The one- and two- metal ion models were presented.<sup>14,15</sup> Current opinion is that metal ions are not directly involved in the cleavage but a metal ion helps to lower pK<sub>a</sub> value of the 2'OH group of G8 and helps to compensate the negative charge of the non-bridging phosphate oxygens.<sup>16</sup> 2'OH group of G8 donates a proton to the leaving group and serves as a general acid. The general base is probably N1 atom of guanine G-12 which is within hydrogen-bonding distance of the 2'-hydroxyl.<sup>17</sup> G-12 has to be either deprotonated on N1-position or it has to be in enol- tautomeric form. If metal ions are involved in the stabilization of these forms of G-12 remains unclear.<sup>14</sup>

Hairpin ribozyme is a small catalytic RNA found in plant RNA viruses. It was discovered in tobacco ringspot virus satellite RNA. The minimal hairpin ribozyme structure consists of four base paired helices and two internal loops. The active site for cleaving is formed with nucleotides from both helices.

The cleavage reaction proceeds by the same way as in the hammerhead ribozyme.<sup>15-18</sup>

The gImS riboswitch deals with the gene encoding glucosamine-6-phosphate (GlcN6P) synthetase. The gImS activity is triggered by binding of the metabolite GlcN6P. Its tertiary structure consists of two helical stacks and the active site adopts a

compact double pseudoknots. The glmS ribozyme is part of class A, the cleavage reactions are very similar as with the hammerhead or hairpin ribozymes, the significant differences are found for protonation of the 5'-oxygen leaving group. This mechanism involves the GlcN6P. The presence of GlcN6C increases the activity about  $10^4$  than without the sugar.<sup>19</sup>

The hepatitis delta virus (HDV) ribozyme is necessary for viral replication. It consists of a double pseudoknot that connects five helical segments. The cleavage mechanism depends on structure of HDV. The activation of the 2'-OH nucleophile is connected with a hydrated  $Mg^{2+}$ . In the crystal structure of an inactive mutant the metal ion binds in the active site.<sup>19</sup> The cleavage of phosphodiester bond takes place due to using an internal nucleophile, the 2'-oxygen of the ribose. The nucleobases in the the ribozyme can participate in acid-base catalysis. The pKa value of cytosine 75 is neutral for the ribozyme-substrate complex and the cytosine in the vicinity of a metal hydroxide acts as a general base catalyst.<sup>20</sup>

The Varkud satellite ribozyme is the largest nucleolytic ribozyme originated from the mitochondria. It consists of five helical section and two three-way junctions. The catalysis requires a divalent cation. The reaction is independent of pH, but the conformation itself can depend on pH. The probably active site is the A730 internal loop.<sup>20</sup>

### **1.7 The Interactions between Metal Ions and Catalytic Nucleic Acids.**

The metal ion interactions with nucleic acids in solution depends on energetic contributions of diffuse and site-bound ions. There are three general types of interactions between metal ions and catalytic nucleic acids (see Figure 12):

1. diffuse binding
2. site-bound outer-sphere binding
3. site-bound inner-sphere binding

Every hydrated metal ion is surrounded by a polarized layer of water molecules that enables diffuse binding interactions with nucleic acids. The negatively charged

phosphate group cause repulsion between nucleotides, but the positively charged metal ions decrease this electrostatic repulsion. The diffusively bound metal ions play a significant role in nucleic acid folding.<sup>13</sup>

The site-bound interactions consists of two different kinds of binding of the metal cation. The site-bound outer-sphere binding interactions are based on interactions without direct contacts of ions and nucleic acids. The metal ion is surrounded by water molecules and via these molecules the metal ion is bound in an outer-sphere manner to nucleic acid. In the large ribosomal subunit a fully hydrated metal cation is located in the major groove and interacts with nucleobase functional groups.<sup>13, 21</sup>

The site-bound inner-sphere binding interactions are based on direct coordination of the metal ion to phosphate oxygens or to N7 and O6 atoms of guanine. This is the result of one metal-bound water replacement by the ligand such as N7 of purines or O6 of guanosine or O4 of uracil.<sup>13,21</sup>

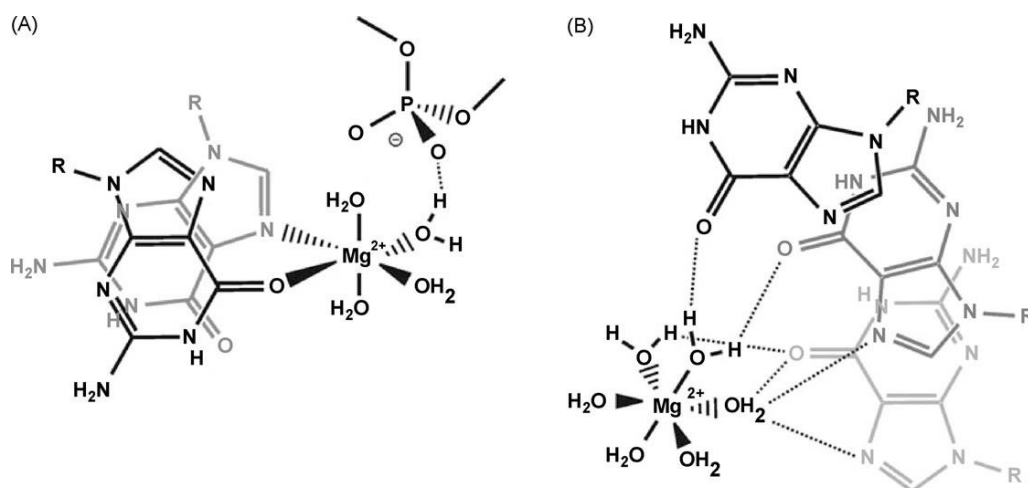


**Fig. 12** Comparison of innersphere and outersphere binding of Mg<sup>2+</sup>. (A) Innersphere , (B) outersphere binding.<sup>21</sup>

### 1.7.1 The Significant Role of Metal Ions in Catalytic Nucleic Acid Reactions

The metal ions play significant structural or catalytic role for the nucleic acids. As we say above, the metal ions influence the folding of the nucleic acids, they reduce the negative charge of phosphodiester bonds and they are mediators of secondary and tertiary interactions of the different blocks of the nucleic acid due to site-bond interactions.<sup>13</sup>

There are five different ways how the metal ions take part in the chemical reactions (see Figure 13). As:

1. general acid catalysts
2. general base catalysts
3. Lewis acids that stabilize the leaving group
4. Lewis acids that enhance the deprotonation of the attacking nucleophile
5. electrophilic catalysts that increases the electrophilicity of the phosphorus atom

ad 1) A metal ion surrounded by water molecules provides proton to the 5'-oxygen leaving group and it acts as a general acid catalyst. This group is also known as M5.

ad 2) A general base catalyst is a metal-coordinated hydroxyl group that causes deprotonation of 2'-OH. This group is also called M2.

ad 3) A metal ion can stabilize the negative charge in the transition state by the coordination of the 5'-oxygen leaving group. This group is also known as M4.

ad 4) A Lewis acid can enhance the deprotonation of the attacking 2'-OH nucleophile, if it coordinates directly with the 2'-oxygen. In the case of the class A the 2'-OH nucleophile is internal, in the case of the class B the nucleophile is external. This group is also known as M1.

ad 5) A metal ion coordinates directly to the non-bridging oxygen. It causes that the phosphorus center is more susceptible to a nucleophilic attack. The metal ion stabilizes the trigonal-bipyramidal transition state. The group is also known as M3.<sup>13,20</sup>

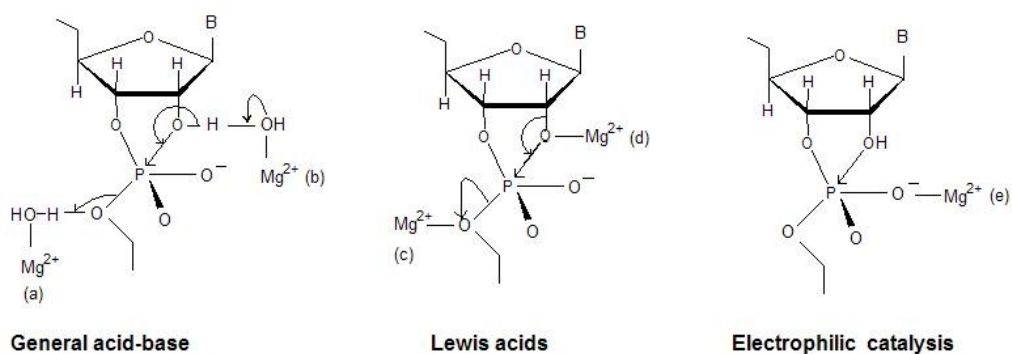


**Fig. 13** Five different ways how the metal ions go into the chemical reactions as: (a) a general acid catalyst, (b) a general base catalyst, (c) A Lewis acid that stabilize the leaving group, (d) a Lewis acid that enhances the deprotonation of the attacking nucleophile, (e) an electrophilic catalyst that increased the electrophilicity of the phosphorus atom.<sup>20</sup>

## 1.8 Tautomerization Process

### 1.8.1 Nucleic Acid Hydration

Hydration is very important for the conformation stability of nucleic acids. B-DNA form has to be strongly hydrated, partial dehydration converts it to A-DNA. In the gas phase or in a non-polar solvent the helical form of nucleic acids is unstable.<sup>22</sup> Nucleic acids have a number of groups with a hydrogen bonding ability towards to water. molecules. RNA is more hydrated than DNA due to existence of unpaired bases and presence of additional O2' oxygen atom. Hydration is greater and more strongly held around the phosphate groups but it is more ordered and more persistent around the bases with their more directional hydrogen-bonding ability.<sup>23</sup> Hydration has a profound influence on the conformation not only of the whole nucleic acids but also of the single nucleotides.<sup>24</sup>

In case of B-DNA both major and minor grooves are hydrated: guanine interacts by N7 and O6 in the major groove and by NH2 and N3 in the minor groove; adenine by N7 and NH2 in the major groove and by N3 in the minor groove; pyrimidines interacts by O2 in the minor groove and by O4 (thymine and uracil if base-paired in RNA) and NH2 (cytosine) in the major groove. Water molecules in the major groove were observed only in low-temperature B-DNA structures obtained in high resolution,

whereas along the minor groove the water molecules are well ordered and connected in the network which is called the spine of hydration.<sup>25</sup> Pyrimidines are usually associated with a single water molecule which forms a hydrogen bond to a neighboring base via a second water molecule forming a water bridge between the two bases.<sup>26</sup> The loss of continuity of the spine of hydration caused by dehydration or cation bindings to the phosphate groups gives rise to the B-DNA  $\rightarrow$  A-DNA transition<sup>27</sup> and it is probably the reason of the higher stability of A-RNA in solutions with high ionic strength (see Figure 14).

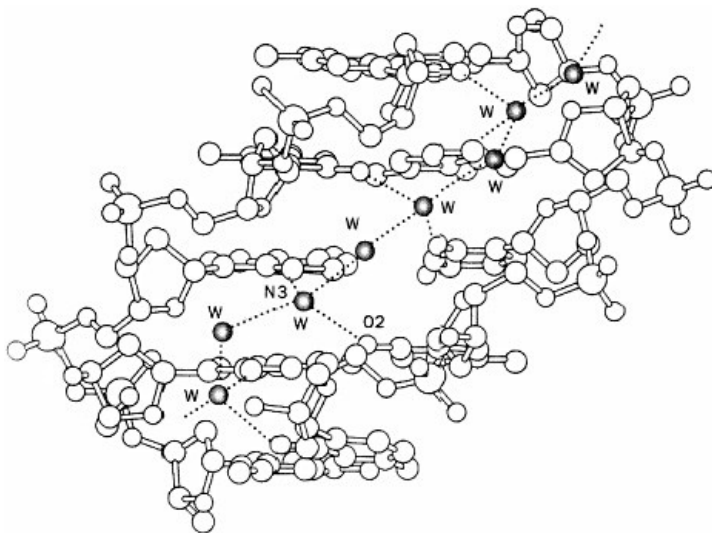


**Fig. 14** Hydration of bases along axis according to Neidle Stephen.<sup>28</sup>

### 1.8.2 Tautomerism of Nucleobases

Tautomerism is a special case of isomerism of organic compounds. The tautomers differ only in the positions of hydrogen atoms therefore tautomerism is caused by a transmigration of a hydrogen atom between the different binding sites. It leads to the bond order changes of corresponding covalent bonds. A single bond switches to a double bond and in the same time another double bond switches to the single bond. The tautomers are in chemical equilibrium which is influenced by many physical and chemical properties such as pH, temperature, presence of external electrostatic fields (presence of charged species) and solvent properties. In nucleic acid bases the most important proton transfers lead to formation of OH and NH<sub>2</sub> groups from keto (=O) and imino (=NH) groups, respectively. These tautomerism shifts are called keto-enol and imino-amino.<sup>11</sup> Tautomerization plays an important role for base-pairing of nucleic acids. Enol tautomers form different H-bonds comparing to canonical keto- tautomers. Therefore when enol tautomer of the base is formed then this base is not able to form Watson-Crick H-bond pattern with the complementary base but stable H-bonds with

another (“incorrect“) base may be established leading to a point mutation.

Surrounding environment affects significantly the chemical equilibrium between tautomers. Different solvents may stabilize different tautomers.<sup>29</sup> For example water molecules may significantly change the relative stabilities of tautomers comparing to the gas phase. The enol form is the most stable tautomer of cytosine in the gas phase but the canonical form is more stable in water since it is much better stabilized in this environment - hydration by just two water molecules is sufficient for this stabilization.<sup>30</sup> Water as a polar solvent stabilizes the better the higher is the dipole moment of a tautomer. In case of guanine it leads to a surprising stabilization of three unusual rare tautomers being energetically comparable to the canonical form in water while being disfavored by about 20 kcal/mol in the gas phase.<sup>31</sup>

The metal ions bind very strongly with nucleic acid bases and affect their keto-enol tautomerism.<sup>10</sup> Beside the phosphate oxygens the main metal binding sites of the metals on nucleobases are N7 and N3 atoms of purines, O6 of guanine and oxo groups of pyrimidines. Metal ion affinity to nucleobases follows the order: G > A > C > T > U.<sup>32</sup> In the first approximation this interaction can be considered as an electrostatic ion – dipole (or induced dipole) interaction but charge transfer and polarization effects are also important.<sup>33,34</sup> The rare tautomers can be stabilized by metal ions and this effect was a subject of a number of studies.<sup>9,29,35</sup> Bare metal ions clearly stabilize tautomers which enable bidentate binding of metal ions to nucleobases. In case of the metal ions under real conditions the situation is much more complicated since the metal ion is hydrated. Every direct coordination binding of the nucleobase to the metal is connected with the nucleobase exchange for one (monodentate binding) or two (bidentate binding) water ligands. When calculating energetic feasibility of this process one has to consider also all possible interactions of the metal ion since these influence the structure of the metal ions' first coordination shell and the strengths of metal ions' coordination bonds. In case of nucleobases the metal ion binding to the negatively charged backbone phosphate can be expected. This interaction is able to suppress the likelihood of the rare tautomer formation.<sup>36</sup>

Some metal ions such as Ni<sup>2+</sup>, Pb<sup>2+</sup>, Cu<sup>2+</sup> and partially also Zn<sup>2+</sup> may act as reduction agents since their second ionization potentials are higher than the first

ionization potentials of the bases. It leads either to the electron transfer from the base to the metal forming ( $M^+-U^+$ ) interaction or to the base deprotonation. In the first case the bond dissociation energies are determined by the value of the second ionization potential of the metal as it was shown for  $Ni^{2+}$ ,  $Cu^{2+}$  and  $Zn^{2+}$ .<sup>9</sup> Association of  $Ni^{2+}$  and  $Zn^{2+}$  ions leads to the stabilization of the keto-enol tautomers.<sup>9</sup> The base deprotonation may occur in the case of  $Pb^{2+}$  and  $Cu^{2+}$  binding.<sup>37,38</sup>

### ***1.8.3 Tautomerism of Uracil***

In vacuum the most stable uracil tautomer has the di-keto form, but if we put near uracil tautomer the magnesium cation, then the most stable tautomer has keto-enol form (the same situation occurs for thymine).

On the base of the theoretical results it is believed that the most stable uracil tautomer is the canonical di-keto tautomer both in the gas phase and in aqueous solution<sup>29</sup> but there is some experimental evidence that rare tautomers may co-exist in the gas phase<sup>39</sup> and in the solution.<sup>40</sup>

Tautomerization process causes changes of the  $\pi$ -electron density that leads to the structural changes of bonds of the pyrimidine ring. Some changes are regular. Two bonds of pyrimidine ring are lengthened and four bonds are shortened. Those lengthened bonds are opposite the transferring proton.<sup>41</sup> The C-O bond, that accepts a proton, is lengthened and the second one is shortened.

The enol form of uracil can be formed by a proton transfer reaction. This proton transfer is very improbable in the gas phase but in water it can be accelerated by a water assisted proton transfer.<sup>7,41</sup> However full hydration of C=O group may decrease the rate of the water assisted proton transfer to form enol C-OH group.<sup>42</sup>

The main difference between canonical di-keto tautomers and rare tautomers is in the nature of functional groups. The di-keto tautomer contains two C=O and N-H groups, while rare tautomers contain combination of C-O-H, C=O, -N- and N-H groups. This changes the hydrogen-bonding pattern and may lead to formation of the complex with other base than adenine.

#### ***1.8.4 The Proton-Transfer Process in a Microhydrated Environment***

Water can be a proton acceptor and a proton donor, the structure in which is water acts as both proton acceptor and donor is energetically favored over the double-donor or double-acceptor structures.<sup>41</sup> However in some complexes the water molecule acts as a bidonor toward the N and O atom and in some complexes the water molecule acts as a biacceptor toward OH and NH groups.<sup>43</sup> These interactions have influence on the tautomerization. Considering the canonical form of uracil (see Figure 16) water acts only as an H-bond donor or only as an H-bond acceptor when bound in regions S4 and S6, respectively. When a water molecule is bound in regions S1, S2 and S3 it acts as both H-bond donor and acceptor. In this case the water molecule is bound in the bidentate binding manner  $N-H \cdots W \cdots O$ . The water accepts the hydrogen atom from the N-H bond of uracil, and in the same time the O atom of uracil accepts hydrogen atom from the water molecule. By this way water molecules can decrease the activation Gibbs free energy of the tautomerization process.<sup>42,44</sup> Kryachko et al.<sup>44</sup> have calculated that importance of  $N-H \cdots O_w$  and  $O_w H_w \cdots O$  H-bonds is the same and they were able to correlate the lengths (and strengths) of these H-bonds with proton affinities and deprotonation enthalpies. In principle whole chain of water molecules, connected by H-bonds to each other, can be involved in the proton transfer forming a proton wire. In ref. 42 the chain up to three water molecules were studied and the assisting tautomerism ability became stronger with increasing number of involved water molecules. On the other hand it was shown that hydration of some binding sites may counteract the tautomerism to some extent.

When considering keto-enol  $\leftrightarrow$  dienol tautomerism it was shown that water molecules always lose their ability to assist the proton transfer increasing the activation Gibbs free energy comparing to the gas phase.<sup>41</sup> It is caused by the small dipole moment of the dienol form that leads to the destabilization in the polar water environment.

#### ***1.8.5 Interaction of Uracil with metal ions with Respect to the Tautomerization Process***

Cations prefer mainly bidentate binding to uracil. The canonical uracil offer only the monodentate binding motif, while the rare tautomers have also the bidentate binding

types. The most favoured binding motif is  $N...Mg^{2+}...O$ .<sup>34</sup> This binding motif is available only in rare enol- tautomers being more stabilized by the metal ion than the canonical form.

For example Wang et al.<sup>45</sup> studied uracil interactions with  $Zn^{2+}$  ion. In the most stable structure  $Zn^{2+}$  ion binds in the bidentate manner to N1 and O2 atoms. The canonical tautomer with the metal bound to O4 is by 22.4 kcal/mol less stable. The same results were also obtained by Marino et al.<sup>32</sup> Monohydration of the  $Zn^{2+}$  ion decreases the difference between the two binding modes by one third to the value of 15.0 kcal/mol. Some studies indicate that the metal cations trigger the tautomerization process, too.<sup>9</sup>

In our study we have focused on the tautomerism of uracil and thymine induced by a proton transfer. We have considered different environments: 1) the gas phase; 2) bare magnesium divalent cation in the gas phase; 3) penta- and hexahydrated magnesium cation in both gas and water; 4) hydrated  $Mg^{2+}$  ion with coordinated phosphate in both gas and water. Thus we were able to characterize quantitatively the influence of the ion coordination (inner and outer) and of the environment on the equilibrium between the tautomers.

## 1.9 The Introduction to Quantum Chemistry and Computational Chemistry

Quantum chemistry is a branch of theoretical chemistry that includes study of electron structure of atoms, molecules and crystal structures and study of their interactions. Quantum chemistry solves the chemistry problems using quantum mechanics and quantum field theory. It determines physical and chemical properties of many electron systems.<sup>46</sup>

Quantum chemistry could be used for interpretation of molecular spectra (electronic, vibrational, rotation spectrum), theoretical predictions of molecular properties, properties of transition states of chemical reactions, intramolecular force determinations, determinations of relative stabilities of molecules, analysis of NMR spectra, mechanisms of chemical reactions.

The Schrödinger's equation for the hydrogen atom offers an exact solution since only two particle (nucleus – electron) problem is described. For many systems with more than one electrons (and protons) two basic approximations are used to solve the Schrödinger's equation: Born-Oppenheimer approximations and orbital approximations. The first approximation enables us to solve nuclear and electron motions independently. Due to the second approximation instead of one many-electron equation we obtain a system of one-electron equations.<sup>46</sup>

### 1.9.1 LCAO - a linear combination of atomic orbitals

LCAO is used for calculating molecular orbitals. The orbitals are expressed as linear combination of basis function - one-electron functions centered on nuclei.

### 1.9.2 The variational method

The variational method is the main approximate method used in quantum chemistry. It is used for finding of the lowest eigenvalue and corresponding eigenvector. Analogical calculations can be obtained by the perturbation method.

The variational theorem includes two parts:

1. Ritz variational theorem

The functional of energy is defined by following formula:

$$E[\Psi] = \langle \hat{H} \rangle_{\Psi} = \frac{\langle \Psi | \hat{H} | \Psi \rangle}{\langle \Psi | \Psi \rangle} ,$$

where  $\hat{H}$  is the Hamiltonian of the system and  $\Psi$  is the arbitrary function of coordinates of the system having finite norm and fulfilling the edge conditions. If we use normalizable wave function  $\langle \Phi | \Phi \rangle = 1$  , then the finding of ground energy level of the system corresponds to minimalization of the functional:

$$E(\phi) = \langle \phi | \hat{H} | \phi \rangle .$$

2. If  $E_0$  is the lowest exact energy  $\hat{H}$  (ground energy level) and corresponding eigenfunction  $\Psi_0$  , then the inequality is:

$$E[\phi] \geq E[\psi_0] = E_0 .$$

The variational principle is possible to generalize for excited states. If the condition  $\langle \psi | \phi \rangle = 0$  is fulfilled, then the following variational principle describes the energy of the first excited state:

$$\frac{\langle \Phi | \hat{H} | \Phi \rangle}{\langle \Phi | \Phi \rangle} \geq E_1 .$$

### ***1.9.3 The Born-Oppenheimer Approximation***

The Born-Oppenheimer Approximation assumes that the solution of time-dependent and time-independent Schrödinger's equation for the many-body systems can be solved due to the separation of the electronic and the nuclear motion in molecules. The wave function of the molecule is described by following formula:

$$\Psi_{total} = \Psi_{electronic} \times \Psi_{nuclear} .$$

The non-relativistic hamiltonian for isolated molecules:

$$\begin{aligned}
\hat{H} &= \hat{T}_e + \hat{T}_n + \hat{V}_{ee} + \hat{V}_{en} + \hat{V}_{nn}, \\
\hat{T}_e &= -\frac{\hbar^2}{2m} \sum_i \Delta_{ri}, \\
\hat{T}_n &= -\frac{\hbar^2}{2} \sum_a \frac{1}{M_a} \Delta_{Ra}, \\
\hat{V}_{ee} &= \frac{e^2}{4\pi\epsilon_0} \sum_{i<j} \frac{1}{r_{ij}}, \\
\hat{V}_{en} &= -\frac{e_2}{4\pi\epsilon_0} \sum_{i,a} \frac{Z_a}{r_{ia}}, \\
\hat{V}_{nn} &= \frac{e_2}{4\pi\epsilon_0} \sum_{a<b} \frac{Z_a Z_b}{R_{ab}},
\end{aligned}$$

where  $\hat{H}_e, \hat{H}_n$  are operators of kinetic energies of electrons and nuclei,  $\hat{V}_{ee}, \hat{V}_{en}, \hat{V}_{nn}$  are operators of potential energies including Coulombic interactions: electron-electron, electron-nucleus, nucleus-nucleus.  $M_a$  and  $Z_a$  is a mass and charge of nucleus  $a$ ,  $m$  is the electron mass,  $r_{ij}$  is a distance between electrons  $i$  and  $j$ ,  $r_{ia}$  is a distance between electron  $i$  and nucleus  $a$ ,  $R_{ab}$  is a distance between nuclei  $a, b$ .

Born and Oppenheimer assumed that kinetic energy of nuclei is a perturbation because the fraction of electron mass and nucleus mass is very small. The velocities of nuclei are insignificant, and kinetic energy of nuclei can be approximated to equate zero. We can study behavior of electrons in a field of frozen nuclei.

The electronic hamiltonian and its corresponding Schrödinger's equation can be calculated by the following formulas:

$$\begin{aligned}
\hat{H}_e &= \hat{T}_e + \hat{V}_{ee} + \hat{V}_{en} + \hat{V}_{nn}, \\
\hat{H}_e \varphi_k(\mathbf{r}; \mathbf{R}) &= E_k^e(\mathbf{R}) \varphi_k(\mathbf{r}; \mathbf{R})
\end{aligned}$$

Then we solve the electronic Schrödinger's equation at frozen nuclear configurations. For example for diatomic molecule, we obtain energy curve - energy as a function of inter-nuclear distance,  $R$ .<sup>46</sup>

There is one question - How significant the error of approximation is? After some sequential correction steps of the Schrödinger's equation shown in ref. 47, we obtain the square matrix  $A_{ji}$  consisting of the system of equations that describe the relationship between electronic and nucleic motion. If all surfaces are separated, the off-diagonal terms can be neglected and the diagonal terms represent the system of the

independent equations:

$$[T_n + \epsilon_j(\mathbf{R})] \Xi_j(\mathbf{R}) = W \Xi_j(\mathbf{R}) ,$$

where  $\epsilon_j(\mathbf{R}) = E_j(\mathbf{R}) - A_{jj}$  is correction to the electronic energy that is obtained from the Born-Oppenheimer approximation. This correction is called the adiabatic correction and it represents the potential field in which the atomic nuclei move.

The Born-Oppenheimer approximation represents very good approximation to the real system. Its error is smaller than errors of other approximations. The Born-Oppenheimer approximation is applied to all quantum chemical calculations of the electronic structure of molecules and solid substances.

#### 1.9.4 Slater Determinant

A Slater determinant is an expression which includes the antisymmetrical factor and satisfies the Pauli exclusion principle. It is used for a description of many-body system - their wavefunction. This determinant assumes that each electron is described by spin-orbital. The spin orbitals are defined as the complete orthonormal systems of one-electron functions  $\lambda_k(\mathbf{x})$  for  $K=1,2,3,\dots$ , which depend on the three dimensional coordinates ( $\mathbf{r}$ ) and the spin coordinate ( $\sigma$ ).

For an N-electron system, the Slater determinant is defined as:

$$\Delta_K(1,2,\dots,n) \equiv \Delta_K(\mathbf{x}_1, \mathbf{x}_2, \dots, \mathbf{x}_n) = \frac{1}{\sqrt{(n!)}} \begin{vmatrix} \lambda_1(\mathbf{x}_1) & \lambda_1(\mathbf{x}_2) & \dots & \lambda_1(\mathbf{x}_n) \\ \lambda_j(\mathbf{x}_1) & & & \lambda_j(\mathbf{x}_n) \\ \vdots & & & \vdots \\ \lambda_u(\mathbf{x}_1) & \lambda_u(\mathbf{x}_2) & \dots & \lambda_u(\mathbf{x}_n) \end{vmatrix} =$$

$$= \frac{1}{\sqrt{(n!)}} \sum_p (-1)^p P \lambda_1(\mathbf{x}_1) \lambda_j(\mathbf{x}_2) \dots \lambda_u(\mathbf{x}_n) = |\lambda_1, \lambda_j, \dots, \lambda_u|$$

The expression  $A = \frac{1}{\sqrt{(n!)}} \sum_p (-1)^p P$  describes the antisymmetrical factor, the term

$\frac{1}{\sqrt{(n!)}}$  is the normalization factor. A single Slater determinant is used as an approximation to the electronic wavefunction in Hartree-Fock theory, it is used for description of many-electron systems.

### 1.9.5 Ab Initio Calculations

The many-electron system can be solved by using different types of approximations. These calculations come from so-called first principles, the Latin term is known as ab initio.<sup>48</sup>

#### 1.9.5.1 Hartree-Fock Theory (SCF)

The Hartree-Fock theory solves N-body wavefunction of the many-body systems by using an approximation obtained by a single Slater determinant or by a single spin-orbitals. The Hartree-Fock theory is based on the variational principle. The Hartree-Fock method is also called the self-consistent field method (SCF).

The many-body system can be expressed as system of one-electron functions which request their own Hamiltonian  $H'$  satisfying an equation  $H'(i)\varphi_i(\mathbf{r}_i)=E_i\varphi_i(\mathbf{r}_i)$ . The function  $\varphi_i(\mathbf{r}_i)$  is called an orbital (atomic or molecular). The orbital can be factorized into a product of one-electron functions:  $\Psi(\mathbf{x})=\lambda_1(\mathbf{x}_1)\lambda_2(\mathbf{x}_2)\dots\lambda_n(\mathbf{x}_n)$ . The function  $\Psi_k$  satisfies the Pauli exclusion principle and represents the diagonal elements of the Slater determinat.

The self-consistent field method requests the functional  $E=\frac{\int \Psi^* H \Psi d\tau}{\int \Psi^* \Psi d\tau}$ .

We find the minimum value of this functional using the Brillouin's theorem. This theorem helps us to formulate the Hartree-Fock equations and the spin-orbitals  $\lambda_k$  can be obtained as a result of these equations.

Finding the Hartree-Fock one-electron wavefunctions is equivalent to the equation:

$\hat{F}(1)\varphi_i(\mathbf{r}_i)=\epsilon_i\varphi_i(\mathbf{r}_i)$  where  $\hat{F}$  is the Fock operator generated by the orbitals  $\varphi_i(\mathbf{r}_i)$  which correspond to one-electron wavefunctions also called the Hartree-Fock molecular orbitals. The equations are solved as a nonlinear problem using iterations. That is why the method is called the self-consistent field method.<sup>47</sup>

### 1.9.5.2 Density Functional Theory (DFT)

The density functional theory is the quantum mechanical theory that investigates the electronic structure of many-body systems. The system properties are determined by using functionals, which depend on the electron density. The determination of non-degenerate ground states depends on the inhomogeneous one-electron density. There are two significant axioms:

1. Total energy of the system of interacting electrons and ions in the explicit position can be obtained from the unique electron-density functional.

2. The functional takes the minimum value for a ground-state density.

The main problem is how to find the explicit form of the functional. Generally we are trying to find the approximate form.

The Kohn-Sham DFT reduces the problem of interacting electrons in a static external potential to the problem of non-interacting electrons moving in an effective potential. The effective potential contains the external potential and terms describing the Coulomb interactions between electrons and the exchange and correlation interactions. The Kohn-Sham equations are very similar to Schrödinger's equation, but they are more complicated because they depend on the electron densities. The results are found by iterative methods and has to be done in a self-consistent way.

The minimum value for functional can be found by the variational principles, from which we obtain the Euler-Lagrange equations (corresponding with K-S equations):

$$\left[ -\frac{\hbar^2}{2m_e} \nabla^2 + v^{\text{ext}}(\mathbf{r}) + e^2 \int \rho \frac{(\mathbf{r}')}{|\mathbf{r}-\mathbf{r}'|} d\mathbf{r}' + \frac{\partial E^{\text{XC}}(\rho)}{\partial \rho} \right] \psi_i(\mathbf{r}) = \epsilon_i \psi_i(\mathbf{r}) ,$$

where  $E^{\text{XC}}$  is functional, the  $v^{\text{ext}}$  is external potential.

The simplest approximation is the local-density approximation(LDA),  $v^{\text{XC}}$ . In this case the functional depends on the density at the coordinate:

$$E^{\text{XC}} = \int v^{\text{XC}}(\mathbf{r}) \rho_e(\mathbf{r}) d\mathbf{r} .$$

The simplest local density approximation was derived by Slater. The non-interacting systems can be expressed by wavefunctions represented by Slater

determinant. The kinetic energy functional is known, the second part - exchange correlation has to be approximated, see above. The exchange-correlation energy density can be derived from quantum Monte Carlo simulations of a free electron model.

For chemical applications a number of exchange-correlation functionals has been developed. The most famous is the BLYP method. The name was originated from the first name letters of four scientist. From the name Becke who developed the exchange part, then Lee, Yang and Parr for the correlation part.

In our study we often use the B3LYP method. It means the Becke 3-Parameter exchange part, Lee, Yang and Parr correlation part. It is a hybrid functional, where exchange energy is obtained from Becke's exchange functional combined with the exact energy from HF theory. A hybrid exchange-correlation function is described as a linear combination of the HF exchange functional and correlation explicit density functionals. The three parameters are predicted and fitted to a system.<sup>48</sup>

## 2 Methods

Starting geometries of all structures were generated with the MOLDEN program.<sup>49</sup> Molden is an interactive visualization program that is capable displaying chemical structures from a number of quantum chemical and semi-empirical packages. It contains also the Z-matrix module that enables preparation of initial geometries of the structures. We prepared all existing tautomers but only the following the most stable structures are analysed – di-keto forms, keto-enol forms and di-enol forms. In case of enol tautomers two different rotamers with the opposite orientation of OH group are distinguished. Quantum chemical calculation were performed with GAUSSIAN 03 (G 03) program.<sup>50</sup> The geometrical and energetical characteristics of tautomers in the gas phase were determined by B3LYP and MP2 methods. For the pre-optimization and the Hessian (zero-point vibration energies) and thermal analysis we adopted the B3LYP/6-31+G\* level of theory using standard G-03 parameters. Then the most stable structures were re-optimized using a larger basis set, 6-311++G\*\*. Single point energy evaluations on the optimized geometries were evaluated with the large basis set 6-311+ +G(2df,2pd) using B3LYP but also MP2 methods. Interaction energies were corrected for the basis set superposition error (BSSE) and the deformation energies of the uracil tautomers according to the following formula:

$$\Delta E_{\text{int}} = E_{\text{complex}} - (E_{\text{base}} + E_{\text{Mg}^{2+}} + BSSE + \Delta E_{\text{def}}) \quad .$$

Relative energies of the tautomers were always calculated with respect to the most stable structure.

### 3 Results

#### 3.1 Tautomerism of uracil

In the Figure 15 thirteen most stable uracil tautomers are presented and their nomenclature is shown, the other less stable tautomers are shown in the supplement.

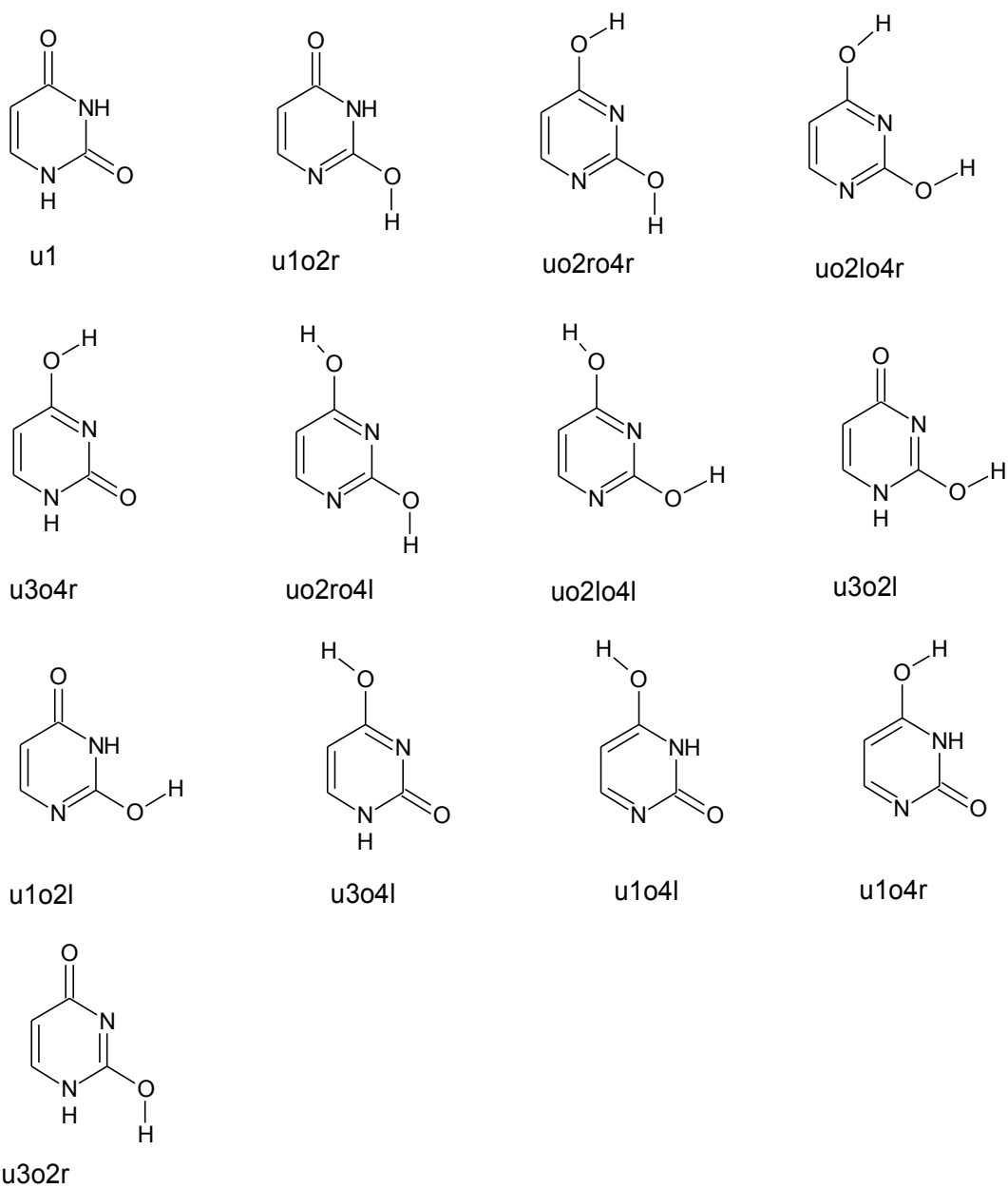


*Fig.15 The thirteen uracil tautomers and their nomenclature.*

**Table 4: Gas phase energies with thermal corrections (in atomic units) of uracil tautomers**

Tautomer	The electronic energy				The corrections				The Gibbs free energy			
	B3LYP		MP2		ZPE	$\Delta U$	$\Delta H$	$\Delta G$	B3LYP		MP2	
	6-31+G*	6-31++G**	6-311++G(2df,2pd)	6-311++G(2df,2pd)					6-31+G*	6-31++G**	6-311++G(2df,2pd)	6-311++G(2df,2pd)
u1	-414.837659	-414.946181	-414.972366	-414.080602	0.087085	0.093268	0.094212	0.056649	-414.781010	-414.889532	-414.915717	-414.023953
u1o2r	-414.817859	-414.927699	-414.954280	-414.064822	0.086649	0.092739	0.093684	0.056418	-414.761441	-414.871281	-414.897862	-414.008404
uo2lo4r	-414.812851	-414.924222	-414.951537	-414.065523	0.086643	0.092621	0.093565	0.056573	-414.756278	-414.867649	-414.894964	-414.008950
uo2lo4r	-414.810944	-414.922321	-414.949765	-414.063743	0.086532	0.092541	0.093486	0.056444	-414.754500	-414.865877	-414.893321	-414.007299
u3o4r	-414.816343	-414.926465	-414.953601	-414.063394	0.086609	0.092715	0.093659	0.056290	-414.760053	-414.870175	-414.897311	-414.007104
uo2o4l	-414.803849	-414.915380	-414.943539	-414.057503	0.086347	0.092410	0.093355	0.056215	-414.747634	-414.859165	-414.887324	-414.001288
uo2lo4l	-414.803812	-414.915296	-414.943389	-414.057374	0.086339	0.092403	0.093347	0.056207	-414.747605	-414.859089	-414.887182	-414.001167
u3o2l	-414.804102	-414.914550	-414.941583	-414.052511	0.086192	0.092488	0.093432	0.055691	-414.748411	-414.858859	-414.885892	-413.998620
u1o2l	-414.804344	-414.914474	-414.942209	-414.052415	0.085808	0.092213	0.093157	0.055281	-414.749063	-414.859193	-414.886928	-413.997134
u3o4l	-414.804647	-414.914942	-414.943205	-414.052798	0.086117	0.092371	0.093316	0.055661	-414.748986	-414.859281	-414.887544	-413.997137
u1o4l	-414.801250	-414.911186	-414.938598	-414.047698	0.085834	0.092117	0.093062	0.055369	-414.745881	-414.855817	-414.883229	-413.992329
u1o4r	-414.796290	-414.906406	-414.934194	-414.042966	0.085284	0.091794	0.092738	0.054584	-414.741706	-414.851822	-414.879610	-413.988382
u3o2r	-414.786389	-414.897266	-414.925851	-414.036371	0.084601	0.090793	0.091737	0.054085	-414.732304	-414.843181	-414.871766	-413.982286

The first column shows the names of the structures. The following four columns summarize the electronic energies obtained at different levels of theory. The columns of the corrections contain Zero-Point Energy Corrections, Thermal correction to Internal Energy, Thermal correction to Enthalpy and Thermal correction to Gibbs Free Energy. In last four columns are summarized absolute Gibbs energies of the structures calculated at different levels of theory.

**Table 5: Gas phase relative energies with thermal corrections (kcal/mol) of uracil tautomers**

Tautomer	The electronic energy				The corrections				The relative Gibbs free energy			
	B3LYP		MP2		$\Delta ZPE$	$\Delta(\Delta H)$	$\Delta(\Delta G)$	$\Delta ZPE$	B3LYP		MP2	
	6-31+G*	6-31++G**	6-311++G(2df,2pd)	6-311++G(2df,2pd)					6-31+G*	6-31++G**	6-311++G(2df,2pd)	6-311++G(2df,2pd)
u1	0.00	0.00	0.00	0.00	0.00	0.00	0.00	0.00	0.00	0.00	0.00	0.00
u1o2r	12.42	11.60	11.35	9.90	-0.27	-0.33	-0.14	-0.28	11.45	11.20	9.76	9.76
uo2lo4r	15.57	13.78	13.07	9.46	-0.28	-0.41	-0.05	-0.35	13.73	13.02	9.41	9.41
uo2lo4r	16.76	14.97	14.18	10.58	-0.35	-0.46	-0.13	-0.35	14.84	14.05	10.45	10.45
u3o4r	13.38	12.37	11.78	10.80	-0.30	-0.35	-0.23	-0.30	12.15	11.55	10.57	10.57
uo2ro4l	21.22	19.33	18.09	14.49	-0.46	-0.54	-0.27	-0.46	19.06	17.82	14.22	14.22
uo2lo4l	21.24	19.38	18.18	14.58	-0.47	-0.54	-0.28	-0.47	19.10	17.91	14.30	14.30
u3o2l	21.06	19.85	19.32	17.63	-0.56	-0.49	-0.60	-0.56	19.25	18.72	17.03	17.03
u1o2l	20.91	19.90	18.92	17.69	-0.80	-0.66	-0.86	-0.80	19.04	18.07	16.83	16.83
u3o4l	20.72	19.60	18.30	17.45	-0.61	-0.56	-0.62	-0.61	18.98	17.68	16.83	16.83
u1o4l	22.85	21.96	21.19	20.65	-0.79	-0.72	-0.80	-0.79	21.16	20.39	19.84	19.84
u1o4r	25.96	24.96	23.95	23.62	-1.13	-0.92	-1.30	-1.13	23.66	22.66	22.32	22.32
u3o2r	32.17	30.69	29.19	27.76	-1.56	-1.55	-1.61	-1.56	29.09	27.58	26.15	26.15

The first column shows the names of the structures. The following four columns summarize the relative energies obtained at different levels of theory. The correction columns refer to the Zero-Point Corrections, Thermal correction to Enthalpy and Thermal correction to Gibbs Free Energy. The last column yields the relative Gibbs free energies.

The most stable tautomer is the u1. This structure is in the di-keto form. The keto-enol tautomers u1o2r, u3o4r and uo2ro4r and uo2lo4r enol-enol tautomers comes after u1 and they are by about 10 kcal/mol less stable. It is in agreement with experimental evidence.<sup>51</sup> The following tautomers are di-enol (uo2lo4l, uo2ro4l) and ket-enol(u3o4l, u3o2l, u1o2l) forms, which are by about 14 and 17 kcal/mol less stable (see Tables 4 and 5). Some structures are rotamers (ou2ro4r and uo2lo4r, u1o4r and u1o4l).

**TABLE 6: Bond distances of thirteen most stable uracil tautomers (at B3LYP/6-31+G\* level of theory)**

Tautomer	N1-C2	C2-N3	N3-C4	C4-C5	C5-C6	C6-N1	N1-H	C2-O2	N3-H	C4-O4	C5-H	C6-H	O2-H	O4-H
u1	1.394	1.385	1.412	1.459	1.352	1.377	1.012	1.220	1.015	1.223	1.082	1.085	-	-
u1o2r	1.302	1.354	1.424	1.449	1.365	1.375	-	1.343	1.016	1.224	1.083	1.087	0.975	-
uo2ro4r	1.355	1.335	1.330	1.403	1.386	1.345	-	1.345	-	1.346	1.083	1.088	0.974	0.976
uo2lo4r	1.329	1.342	1.332	1.400	1.389	1.343	-	1.346	-	1.347	1.083	1.088	0.973	0.975
u3o4r	1.423	1.380	1.308	1.430	1.363	1.358	1.013	1.221	-	1.345	1.081	1.085	-	0.977
uo2ro4l	1.339	1.332	1.326	1.407	1.388	1.341	-	1.345	-	1.352	1.085	1.088	0.974	0.971
uo2lo4l	1.333	1.339	1.328	1.404	1.391	1.339	-	1.345	-	1.352	1.085	1.088	0.974	0.971
u3o2l	1.411	1.388	1.443	1.518	1.330	1.502	1.011	1.378	-	1.207	1.087	1.086	0.965	-
u1o2l	1.297	1.365	1.429	1.443	1.367	1.372	-	1.348	1.016	1.225	1.083	1.087	0.971	-
u3o4l	1.428	1.377	1.303	1.437	1.364	1.353	1.013	1.220	-	1.353	1.084	1.085	-	0.971
u1o4l	1.381	1.435	1.349	1.376	1.419	1.314	-	1.219	1.015	1.347	1.084	1.091	-	0.971
u1o4r	1.375	1.442	1.355	1.375	1.415	1.317	-	1.219	1.015	1.346	1.082	1.090	-	0.972
u3o2r	1.380	1.282	1.410	1.475	1.347	1.389	1.011	1.354	-	1.224	1.083	1.084	0.970	-
u13o2r	1.325	1.320	1.526	1.449	1.343	1.465	1.015	1.343	1.018	1.212	-	1.088	0.973	-
u13o2l	1.321	1.324	1.541	1.444	1.349	1.448	1.015	1.344	1.018	1.213	-	1.089	0.974	-
u3o2lo4r	1.339	1.311	1.365	1.419	1.367	1.408	1.016	1.344	-	1.342	-	1.089	0.975	0.975

*B3LYP/6-31+G\* optimized bond distances of ten most stable uracil tautomers (the upper part of the Table). Three tautomers in the bottom part of the Table are substantially less stable but they are also presented here since they are stabilized in the presence of a metal ion. See Figure 16 for numbering of bonds.*

### 3.2 Mg<sup>2+</sup> Binding to All Tautomers of Uracil

We concern about the binding sites of the magnesium ion on the tautomers of uracil we have studied in the previous section. . Supposing that the metal lies in the plane of uracil we can divide the plane to the six sections (S1-S6) to which every binding site can be assigned (Figure 16). We prepared z - matrixes of metalated tautomers of uracil (we considered all possible binding sites S1 - S6) and optimized these structures using G 03. In some sections we were not able to find any stable binding site and the metal ion moved into another section with a stable binding site during the optimization (Figure 17).

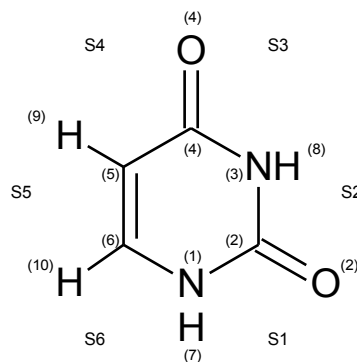


**Figure 16:** All binding sites of magnesium ion in the vicinity of uracil. I used standard numbering of atoms.

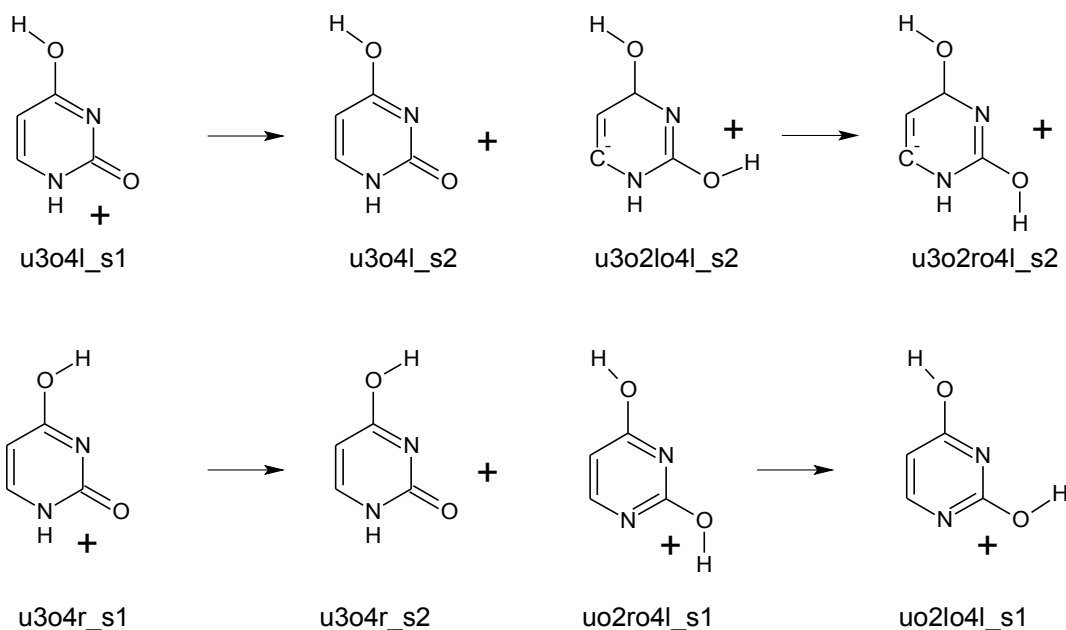


**Fig. 17** Some examples of unstable structures. In these cases the instability is caused by the clash between the metal cation and a hydrogen atom. It leads to the metal ion movement (in case of u3o4l\_s1, u3o4r\_s1) or a formation of a more feasible rotamers (in case of u3o2lo4l\_s2, uo2ro4l\_s1).

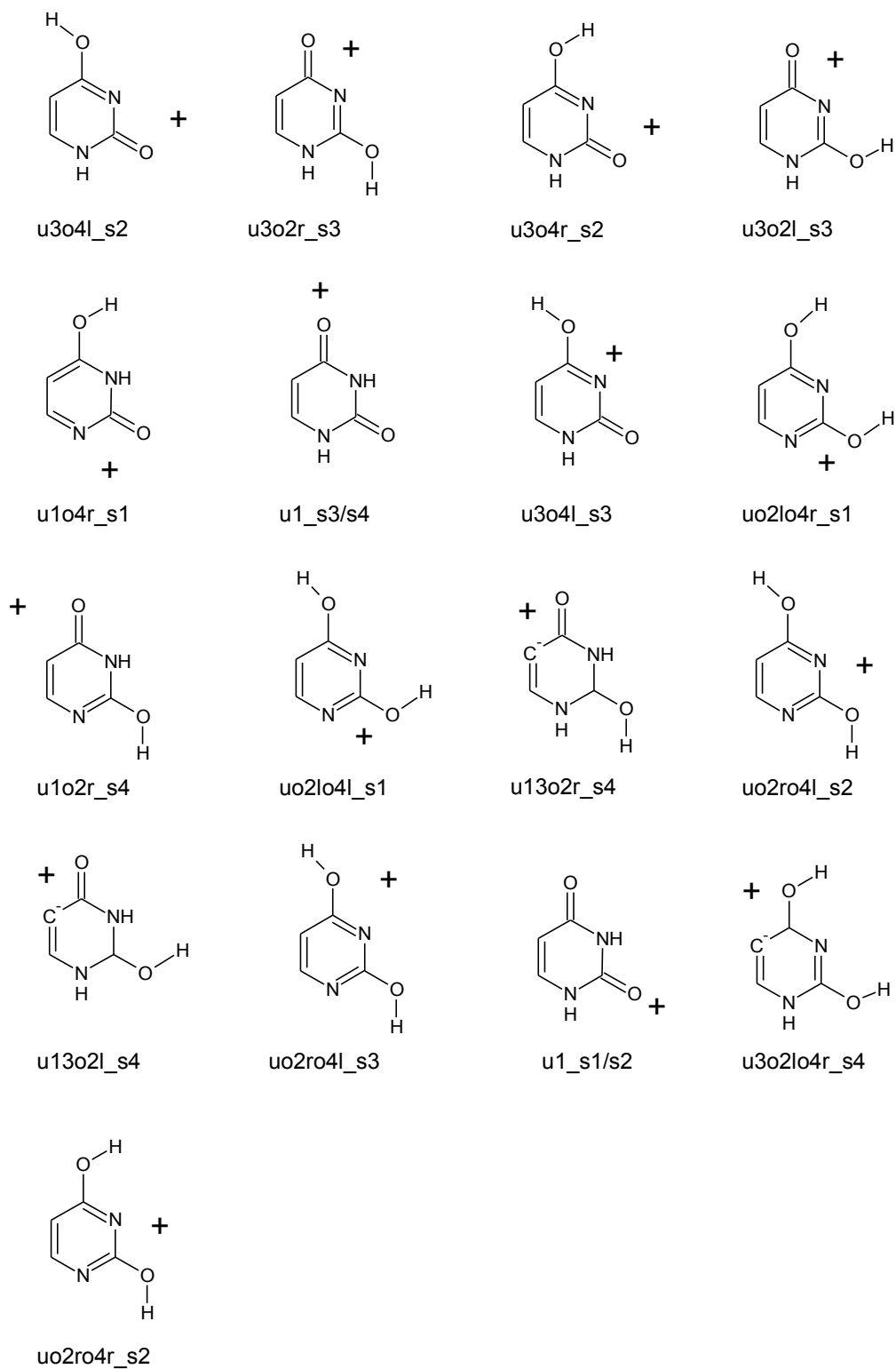


**Fig. 18** The seventeen most stable metalated tautomers of uracil. The position of the  $Mg^{2+}$  metal ion is indicated by a cross. Standard numbering and nomenclature are presented.

Table 7: Gas phase energies with thermal corrections (in atomic units) of uranyl tautomers with bound magnesium ions

Name	The electronic energy			The corrections				The Gibbs free energy		
	B3LYP			ZPE	$\Delta U$	$\Delta H$	$\Delta G$	B3LYP		
	6-31+G*	6-311++G**	6-311++G(2d(2,pd)					6-31+G*	6-311++G**	6-311++G(2d(2,pd)
u3o4l_s2	-614.320717	-614.441873	-614.474929	0.096867	0.097811	0.057815	-614.262902	-614.384058	-614.417114	-613.093783
u3o2l_s3	-614.312449	-614.433683	-614.467238	0.089706	0.089706	0.057087	-614.255362	-614.374732	-614.410151	-613.086854
u3o4r_s2	-614.310867	-614.431967	-614.465494	0.089255	0.096569	0.097513	-614.253632	-614.374732	-614.408259	-613.084877
u3o2l_s3	-614.309872	-614.430908	-614.464419	0.089088	0.096439	0.097384	-614.252903	-614.373939	-614.407450	-613.083845
u1o4r_sl	-614.308867	-614.430041	-614.463703	0.089040	0.096322	0.097266	-614.251795	-614.372969	-614.406631	-613.082621
u1_s3/s4	-614.285165	-614.407006	-614.437393	0.089063	0.096871	0.097815	-614.229728	-614.351569	-614.381956	-613.058262
u3o4l_s3	-614.280477	-614.404253	-614.433372	0.088323	0.095954	0.096898	-614.224608	-614.348384	-614.377503	-613.055575
u2o2o4r_sl	-614.277912	-614.402903	-614.433462	0.088189	0.095591	0.096536	-614.221802	-614.346793	-614.373732	-613.058634
u1o2l_s4	-614.273783	-614.396490	-614.427900	0.088560	0.096307	0.097251	-614.218704	-614.341411	-614.372821	-613.051233
u13o2l_s4	-614.273452	-614.396447	-614.429684	0.089222	0.096646	0.097391	-614.216267	-614.339262	-614.372499	-613.046463
u2o2o4l_sl	-614.273252	-614.398237	-614.429309	0.088195	0.095587	0.096531	-614.217130	-614.342115	-614.373187	-613.054439
u13o2l_s4	-614.273189	-614.396190	-614.429311	0.089161	0.096609	0.097554	-614.216089	-614.339090	-614.372211	-613.046017
u2o2o4l_s2	-614.269410	-614.394098	-614.427724	0.088008	0.095443	0.096387	-614.213455	-614.338143	-614.371769	-613.048409
u2o2o4l_s3	-614.269405	-614.394098	-614.424046	0.087983	0.095381	0.096325	-614.213684	-614.338377	-614.368325	-613.048642
u1_s1/s2	-614.267418	-614.389641	-614.420016	0.088255	0.096278	0.097222	-614.213035	-614.335258	-614.365633	-613.043996
u3o2o4r_s4	-614.261024	-614.368871	-614.417059	0.088757	0.096263	0.097207	-614.204479	-614.330326	-614.360514	-613.037165
u2o2o4r_s2	-614.258050	-614.383150	-614.414041	0.087363	0.094944	0.095889	-614.202945	-614.328045	-614.358936	-613.040515

The first column corresponds to the name of the structure. The following four columns summarize the energies obtained at different levels of theory. The columns of the corrections are supposed to correct the electronic energies. The view columns contains information about Zero-Point Corrections, Thermal correction to Enthalpy, and Thermal correction to Gibbs Free Energy.

Table 8: Gas phase relative energies with thermal corrections (kcal/mol) of uranyl tautomers with bound magnesium ions

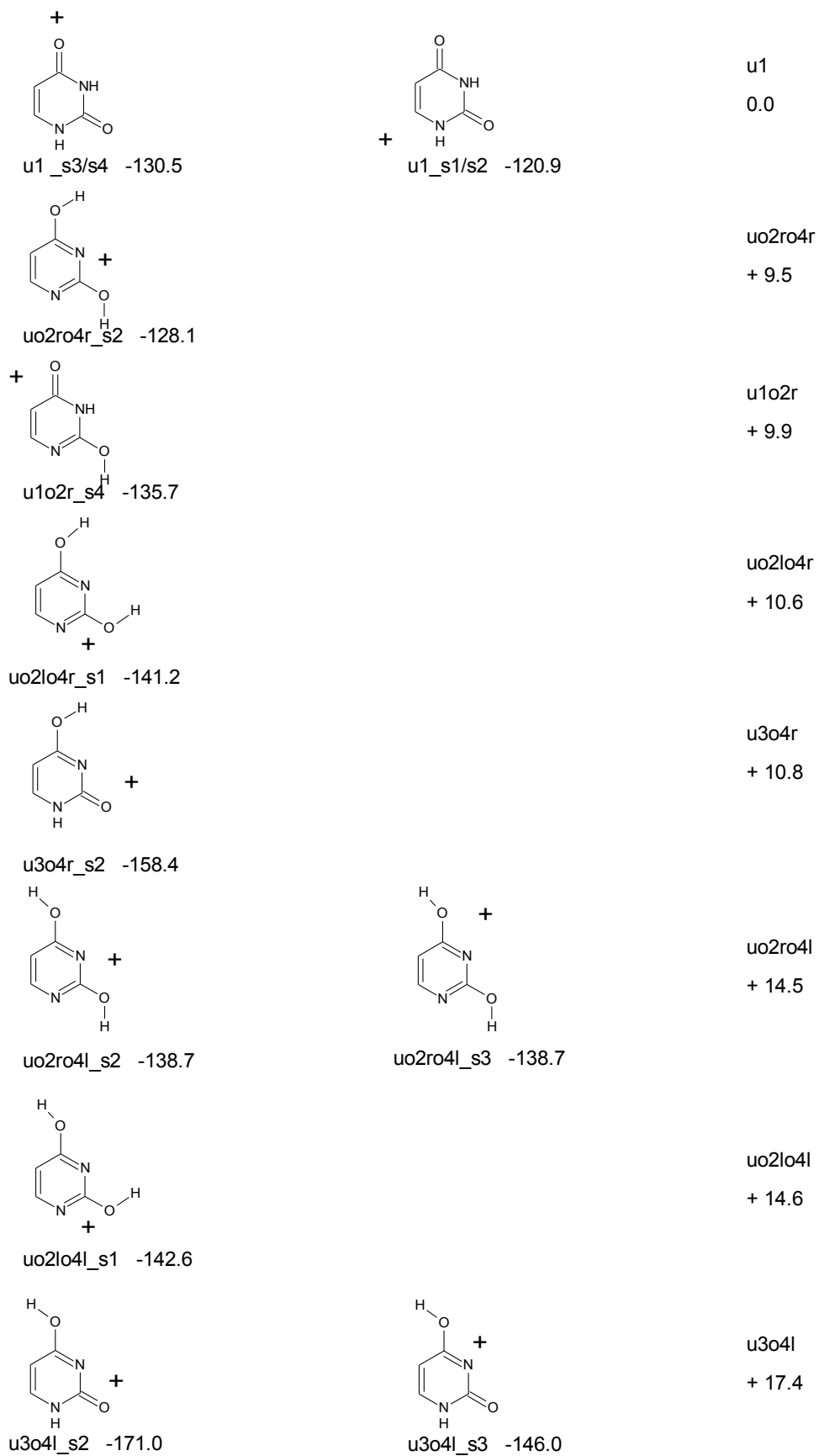
Tautomer	The electronic energy			The corrections				The relative Gibbs free energy		
	B3LYP			$\Delta ZPE$	$\Delta U/\Delta H$	$\Delta G/\Delta G$	B3LYP			
	6-31+G*	6-311++G**	6-311++G(2d(2,pd)				6-31+G*	6-311++G**	6-311++G(2d(2,pd)	
u3o4l_s2	0.00	0.00	0.00	0.00	0.00	0.00	0.00	0.00	0.00	0.00
u3o2r_s3	5.19	4.83	4.80	-0.38	-0.27	-0.46	4.73	4.68	4.37	4.35
u3o4r_s2	6.18	5.92	5.95	-0.26	-0.19	-0.36	5.82	5.85	5.56	5.59
u3o2l_s3	6.81	6.60	6.77	-0.39	-0.27	-0.53	6.27	6.35	6.06	6.24
u1o4r_sl	7.44	7.04	7.47	-0.42	-0.34	-0.47	6.97	6.96	6.58	7.00
u1_s3/s4	22.31	21.88	23.78	-0.40	0.00	-1.49	20.82	20.39	22.06	22.29
u3o4l_s3	25.25	23.61	26.08	-0.87	-0.57	-1.22	24.03	22.39	24.86	23.98
u2o2o4r_sl	26.86	24.45	26.02	-0.95	-0.80	-1.07	25.79	23.38	24.95	22.06
u1o2r_s4	29.45	28.48	29.51	-0.72	-0.35	-1.72	27.73	26.76	27.79	26.70
u13o2l_s4	29.66	28.51	28.39	-0.30	-0.14	-0.40	29.26	28.11	28.00	29.69
u2o2o4l_sl	29.78	27.38	28.63	-0.95	-0.80	-1.06	28.72	26.32	27.56	24.69
u13o2l_s4	29.82	28.67	28.63	-0.34	-0.16	-0.45	29.38	28.22	28.18	29.97
u2o2o4l_s2	32.20	29.98	29.62	-1.06	-0.89	-1.17	31.03	28.81	28.45	28.47
u2o2o4l_s3	32.20	29.98	29.64	-1.14	-0.93	-1.31	30.88	28.67	30.62	28.33
u1_sl/s2	33.45	32.78	34.46	-0.91	-0.37	-2.15	31.29	30.62	32.30	31.24
u3o2o4r_s4	37.46	34.51	36.31	-0.59	-0.38	-0.80	36.66	33.72	35.52	35.53
u2o2o4r_s2	39.32	36.85	38.21	-1.47	-1.21	-1.70	37.62	35.15	36.51	33.43

The first column shows the names of the structures. The following four columns summarize relative energies obtained at different levels of theory. They are given with respect to the most stable u3o4l\_s2 structure. The correction columns refer to the Zero-Point Corrections, Thermal correction to Enthalpy, and Thermal correction to Gibbs Free Energy. The Thermal correction to Energy is not included, its value is identical with the Thermal correction to Enthalpy. The second part of the table gives relative Gibbs Free Energies obtained as the sum of calculated electronic energies and of all corrections.

**Table 9: Uracil ... Mg<sup>2+</sup> interaction gas phase energies**

Structure	E <sub>comp</sub>	E <sub>Udef</sub>	E <sub>Uned</sub>	BSSE	E <sub>Def</sub>	E <sub>int</sub>
u3o4l_s2	-613.151598	-414.037410	-414.052798	2.13	9.66	-170.95
u3o2r_s3	-613.143941	-414.022534	-414.036371	2.08	8.68	-176.50
u3o4r_s2	-613.142112	-414.047075	-414.063394	2.06	10.24	-158.40
u3o2l_s3	-613.140814	-414.038014	-414.052511	2.00	9.10	-164.48
u1o4r_s1	-613.139693	-414.025944	-414.042966	2.06	10.68	-169.71
u1_s3/s4	-613.113699	-414.064407	-414.080602	1.37	10.16	-130.47
u3o4l_s3	-613.111444	-414.039282	-414.052798	1.87	8.48	-146.01
uo2lo4r_s1	-613.114744	-414.049071	-414.063743	1.84	9.21	-141.24
u1o2r_s4	-613.106312	-414.047684	-414.064822	1.41	10.75	-135.70
u13o2r_s4	-613.103648	-413.929628	-413.946491	2.03	10.58	-207.66
uo2lo4l_s1	-613.110561	-414.042864	-414.057374	1.82	9.11	-142.63
u13o2l_s4	-613.103117	-413.931118	-413.948643	2.05	11.00	-205.96
uo2ro4l_s2	-613.104364	-414.044122	-414.057503	1.83	8.40	-138.65
uo2ro4l_s3	-613.104363	-414.044134	-414.057503	1.83	8.39	-138.65
u1_s1/s2	-613.098379	-414.063411	-414.080602	1.34	10.79	-120.89
u3o2lo4r_s4	-613.093710	-413.962322	-413.974656	1.80	7.74	-183.98
uo2ro4r_s2	-613.095620	-414.050074	-414.065523	1.85	9.69	-128.11

All energies were calculated at MP2/6-311++G(2df,2pd)//B3LYP-6-311++G\*\* level of theory. The total energy of the uracil...Mg<sup>2+</sup> complex is shown in second column. Energies of uracil tautomers are shown in the third column, the fourth column shows energies of uracil tautomers with the 'ghost' functions on the magnesium ion. The total energy of the Mg<sup>2+</sup> ion is -198.822994 a.u. All these energies are expressed in atomic units. The deformation energies (E<sub>def</sub>) in the sixth column were calculated as a difference of total energies of uracil tautomers in optimized geometries and geometries in the complex. The last column summarizes the interaction energies.



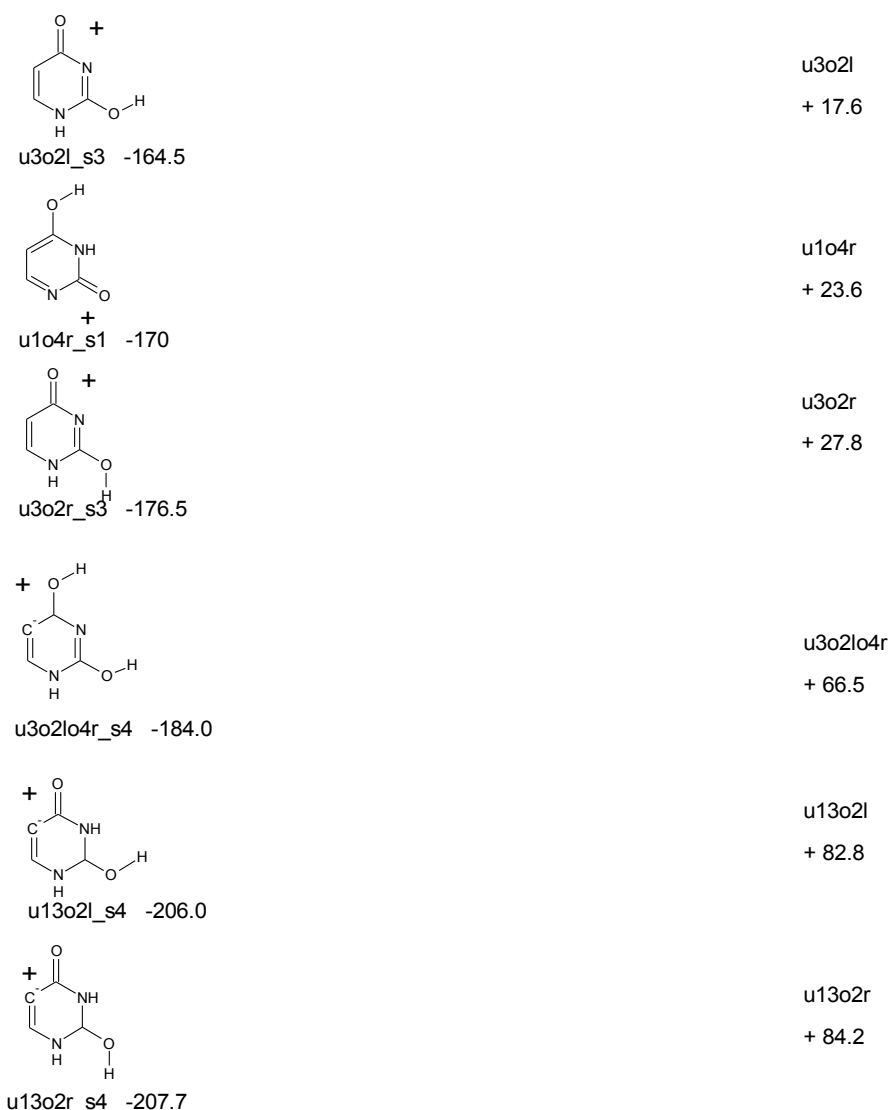


**Fig. 19** Schematic drawings of the optimized uracil...Mg<sup>2+</sup> complexes. At the bottom of each structure the stabilization energy for Mg<sup>2+</sup> (in kcal/mol) is shown. The relative energies of the tautomers in respect to the canonical u1 form are written at the right edge.

The most stable metalated uracil tautomer is denoted as u3o4l\_s2. This structure refers to the keto-enol form and the magnesium is located on the second binding site (for short: S2, see figure 18) and it is bound in the bidentate manner forming O2-Mg-N3 bridge.. The O4-H group at the opposite orientation with respect to the metal ion to decrease a not feasible Mg<sup>2+</sup>...H interaction.

The second most stable structure u3o2r\_s3 is also the keto-enol tautomer. In this case the magnesium ion is located in the S3 region and it forms bidentate O4-Mg-N3 bond. OH group is located on O2 oxygen and also in this case it has the opposite orientation with respect to the metal ion. But why the u3o2r\_s3 structure is by 4.35 kcal/mol less

stable than the u3o4l\_s2 structure? It is probably caused by the presence of the hydrogen atom on N1. This hydrogen is acidic (Miller 2004) and in the former structure it is closer to the metal ion that destabilizes this structure.

U3o4r\_s2 and u3o2l\_s3 are rotamers of u3o4l\_s2 and u3o2r\_s3 structures. The O2-H group has less feasible orientation with smaller  $Mg^{2+}\cdots H(O2)$  distances in the former structures that leads to the destabilizations of 5.59 and 1.89 kcal/mol of u3o4r\_s2 and u3o2l\_s3 structures with respect to u3o4l\_s2 and u3o2r\_s3 structures, respectively.

U1o4r\_s1 is the keto-enol tautomer, it is the most stable structure that has the hydrogen atom on N3. No hydrogen is bound on N1 atom. Magnesium ion is located on S1 site forming N1-Mg-O2 bidentate bond. The structure is by 7 kcal/mol less stable than the u3o4l\_s2.

The structure u1\_s3/s4 goes down to the sixth place, despite the fact that u1 is the most stable tautomer of the bare uracil. U1\_s3/s4 is the di-keto tautomer. The magnesium binds to oxygen O4 in a monodentate manner and it is a reason of its decreased stability since bidentate binding has a stronger stabilizing effect.

The structure uo2lo4r\_s1 is the most stable di-enol tautomer. Overall uo2lo4r\_s1 ranks the seventh place. Magnesium binds by bidentate manner to N1 and O2 atoms but interaction of magnesium with hydroxo O2-H group is less advantageous than with the keto group. The only feasible orientation of the O2-H group is the opposite orientation with respect to the metal ion – see uo2lo4l\_s1 → uo2lo4r\_s1 transition in Figure 17.

U3o4l\_s3 differs from the most stable tautomer u3o4l\_s2 only by the position of the magnesium ion. The destabilization by 23.98 kcal/mol of the former structure is caused by less effective interaction with the hydroxo O4-H group instead with the keto group on the O2 atom.

Uo2lo4l\_s1 is a less stable rotamer of uo2lo4r\_s1. The orientation of O4-H group leads to destabilization of 2.6 kcal/mol of uo2lo4l\_s1 with respect to uo2lo4r\_s1. Energy difference between the two structures is slightly smaller than energy difference between the corresponding tautomers (uo2lo4l and uo2lo4r) in absence of magnesium ion (see Table 5).

In u1o2r\_s4 structure the magnesium ion is bound to O4 but on the site S4, i.e. it shows some interaction with non-polar C5-H group. This metal conformation is more feasible since site S3 is occupied by the polar N3-H bond. Therefore H(N3) hydrogen is more acidic and it bears higher positive charge than H(C5) hydrogen.

The eleventh most stable structure u13o2r\_s4 was created by deprotonation of the C5 carbon (see also structures u13o2l\_s4 and u3o2lo4r\_s4). Carbon C5 is charged negatively. U13o2r\_s4 is keto-enol tautomer which O2 atom is protonized. The structure is very similar to u1o2r\_s4, the difference of energy is only 2.99 kcal/mol showing that a metal ion can stabilize the negative charge on C5 (note that in absence of the metal ion u13o2r tautomer is by 74.3 kcal/mol less stable than u1o2r).

Uo2ro4l\_s3 and uo2ro4l\_s2 are di-enol tautomers with the N-Mg-OH binding motif. In the uo2ro4l\_s3 structure magnesium ion is bound N3 and O4 and this structure is by 0.15 kcal/mol more stable than the uo2ro4l\_s2 structure where magnesium ion binds to N3 and O2.

U13o2l\_s4 is the keto-enol tautomer with deprotonized carbon C5 and two N-H groups. This structure is the less stable rotamer of u13o2r\_s4.

U1\_s1/s2 is the second most stable di-keto complex. The electronegative oxygen O2 oxygen attracts the magnesium ion, but the interaction is negatively influenced by two nearby NH groups.

Uo2ro4r\_s2 is the rotamer of uo2ro4l\_s2. The opposite orientation of the O4-H group increases inconvenient interaction between H(O2) and  $Mg^{2+}$  that leads to the destabilization of 4.95 kcal/mol with respect to uo2ro4l\_s2.

The structure u3o2lo4r\_s4 is the di-enol tautomer, where magnesium cation is bound to the deprotonized C5 and O4. Negative charge on oxygen O4 is more delocalized due to the bound proton comparing to the keto-form.

The general law for the stability of metalated uracil tautomers is summarized hereinafter: The magnesium ion prefers bidentate binding sites with the N-Mg-O binding motif. Bidentate binding to the N-Mg-OH binding motif and monodentate binding to the keto group are less stable. Stability of tautomers is also influenced by not feasible  $Mg^{2+}-H^{(\delta+)}$  interactions (see Figure 19).

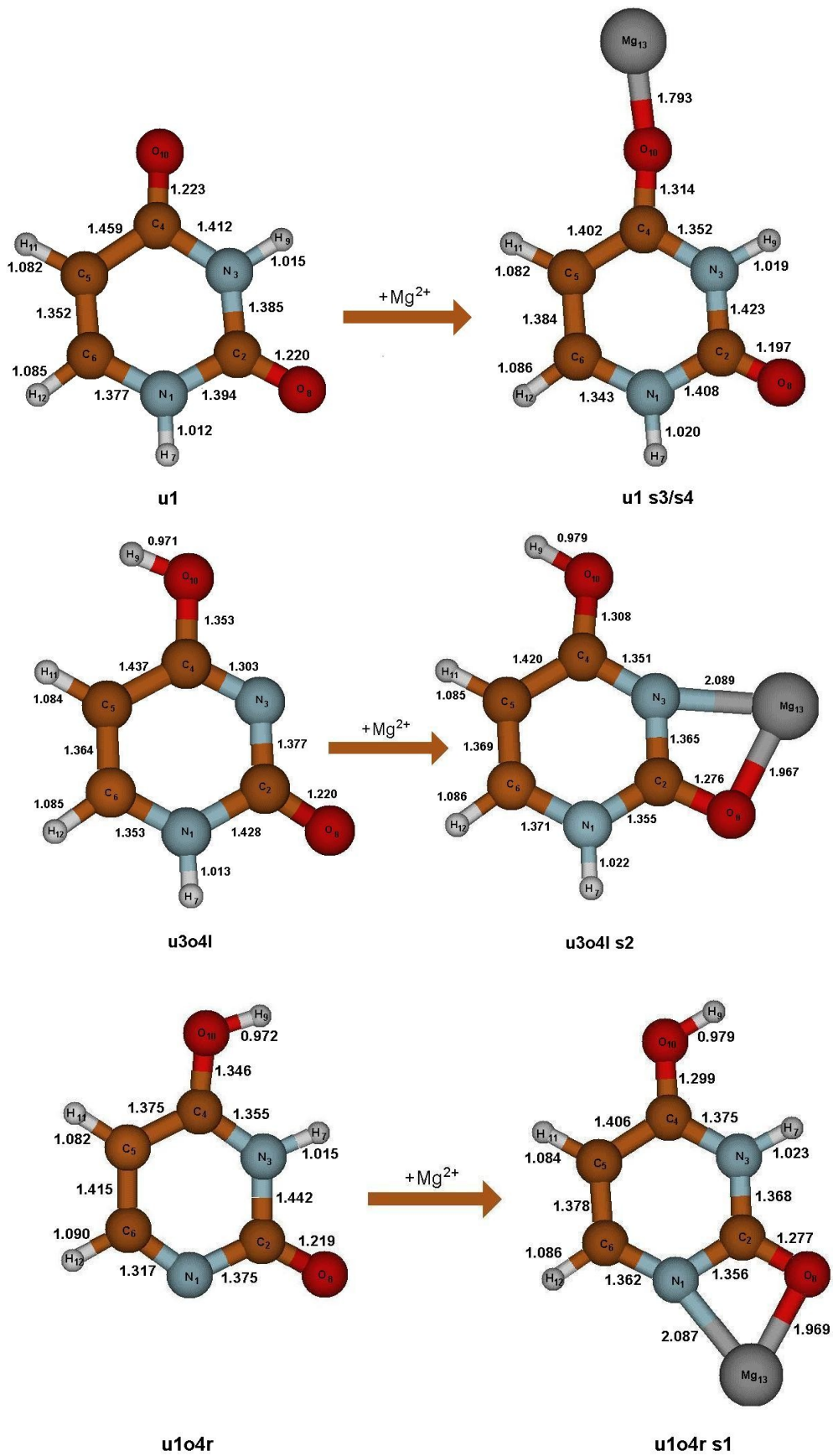
**Table 10: Geometrical parameters calculated in the gas phase for seventeen most stable structures (see Figure 16 for numbering of bonds).**

Tautomers	N1-C2	C2-N3	N3-C4	C4-C5	C5-C6	C6-N1	N1-H	C2-O2	N3-H	C4-O4	C5-H	C6-H	O2-H	O4-H	N1-Mg	O2-Mg	N3-Mg	O4-Mg	C5-Mg
u3o4l_s2	1.355	1.365	1.351	1.420	1.369	1.371	1.022	1.276	-	1.308	1.085	1.086	-	0.979	-	1.967	2.089	-	-
u3o2r_s3	1.353	1.330	1.391	1.425	1.361	1.395	1.020	1.308	-	1.278	1.084	1.086	0.978	-	-	-	2.097	1.947	-
u3o4r_s2	1.349	1.373	1.358	1.421	1.364	1.375	1.022	1.280	-	1.305	1.084	1.086	-	0.976	-	1.934	2.138	-	-
u3o2l_s3	1.352	1.335	1.401	1.419	1.364	1.374	1.022	1.306	-	1.281	1.084	1.086	0.975	-	-	-	2.141	1.920	-
u1o4r_s1	1.356	1.368	1.375	1.406	1.378	1.362	-	1.277	1.023	1.299	1.084	1.086	-	0.979	2.087	1.969	-	-	-
u1_s3/s4	1.408	1.423	1.352	1.402	1.384	1.343	1.020	1.197	1.019	1.314	1.082	1.086	-	-	-	-	-	1.793	-
u3o4l_s3	1.423	1.407	1.336	1.382	1.398	1.337	1.022	1.200	-	1.388	1.083	1.087	-	0.981	-	-	1.990	2.153	-
uo2lo4r_s1	1.344	1.291	1.360	1.423	1.370	1.378	-	1.400	-	1.300	1.085	1.085	0.983	0.981	2.018	2.045	-	-	-
u1o2r_s4	1.315	1.370	1.369	1.387	1.403	1.338	-	1.309	1.020	1.318	1.083	1.087	0.981	-	-	-	-	1.793	-
u13o2r_s4	1.338	1.352	1.386	1.440	1.353	1.409	1.020	1.298	1.025	1.263	-	1.086	0.979	-	-	-	-	2.040	2.115
uo2lo4l_s1	1.348	1.284	1.359	1.425	1.374	1.373	-	1.402	-	1.303	1.085	1.085	0.984	0.978	2.019	2.036	-	-	-
u13o2l_s4	1.338	1.363	1.396	1.435	1.357	1.397	1.022	1.298	1.023	1.264	-	1.086	0.979	-	-	-	-	2.049	2.112
uo2ro4l_s2	1.283	1.352	1.360	1.408	1.387	1.367	-	1.401	-	1.315	1.086	1.087	0.984	0.978	-	2.050	2.019	-	-
uo2ro4l_s3	1.327	1.359	1.353	1.367	1.419	1.330	-	1.311	-	1.397	1.085	1.088	0.982	0.981	-	-	2.015	2.080	-
u1_s1/s2	1.340	1.330	1.478	1.458	1.346	1.404	1.015	1.308	1.018	1.199	1.084	1.084	-	-	-	1.804	-	-	-
u3o2lo4r_s4	1.363	1.332	1.315	1.409	1.375	1.368	1.023	1.300	-	1.380	-	1.086	0.981	0.983	-	-	-	-	2.076
uo2ro4r_s2	1.277	1.365	1.369	1.411	1.379	1.371	-	1.407	-	1.310	1.085	1.086	0.984	0.974	-	1.992	2.052	-	-

**Table 11 Changes of bond distances caused by Mg2+ binding (differences between the structures with and without**

**Mg2+ ion are shown – compare Table 6 and 10).**

Tautomers	N1-C2	C2-N3	N3-C4	C4-C5	C5-C6	C6-N1	N1-H	C2-O2	N3-H	C4-O4	C5-H	C6-H	O2-H	O4-H
u3o4l_s2	-0.073	-0.012	0.048	-0.017	0.005	0.018	0.009	0.056	-	-0.045	0.001	0.001	-	0.008
u3o2r_s3	-0.027	0.048	-0.019	-0.050	0.014	0.006	0.009	-0.046	-	0.054	0.001	0.002	0.008	-
u3o4r_s2	-0.074	-0.007	0.050	-0.009	0.001	0.017	0.009	0.059	-	-0.040	0.003	0.001	-	-0.001
u3o2l_s3	-0.059	-0.053	-0.042	-0.099	0.034	-0.128	0.011	-0.072	-	0.074	-0.003	0.000	0.010	-
u1o4r_s1	-0.019	-0.074	0.020	0.031	-0.037	0.045	-	0.058	0.008	-0.047	0.002	-0.004	-	0.007
u1_s3/s4	0.014	0.038	-0.060	-0.057	0.032	-0.034	0.008	-0.023	0.004	0.091	0.000	0.001	-	-
u3o4l_s3	-0.005	0.030	0.033	-0.055	0.034	-0.016	0.009	-0.020	-	0.035	-0.001	0.002	-	0.010
uo2lo4r_s1	0.015	-0.051	0.028	0.023	-0.019	0.035	-	0.054	-	-0.047	0.002	-0.003	0.010	0.006
u1o2r_s4	0.013	0.016	-0.055	-0.062	0.038	-0.037	-	-0.034	0.004	0.094	0.000	0.000	0.006	-
u13o2r_s4	0.013	0.032	-0.140	-0.009	0.010	-0.056	0.005	-0.045	0.007	0.051	-	-0.002	0.006	-
uo2lo4l_s1	0.015	-0.055	0.031	0.021	-0.017	0.034	-	0.057	-	-0.049	0.000	-0.003	0.010	0.007
u13o2l_s4	0.017	0.039	-0.145	-0.009	0.008	-0.051	0.007	-0.046	0.005	0.051	-	-0.003	0.005	-
uo2ro4l_s2	-0.056	0.020	0.034	0.001	-0.001	0.026	-	0.056	-	-0.037	0.001	-0.001	0.010	0.007
uo2ro4l_s3	-0.012	0.027	0.027	-0.040	0.031	-0.011	-	-0.034	-	0.045	0.000	0.000	0.008	0.010
u1_s1/s2	-0.054	-0.055	0.066	-0.001	-0.006	0.027	0.003	0.088	0.003	-0.024	0.002	-0.001	-	-
u3o2lo4r_s4	0.024	0.021	-0.050	-0.010	0.008	-0.040	0.007	-0.044	-	0.038	-	-0.003	0.006	0.008



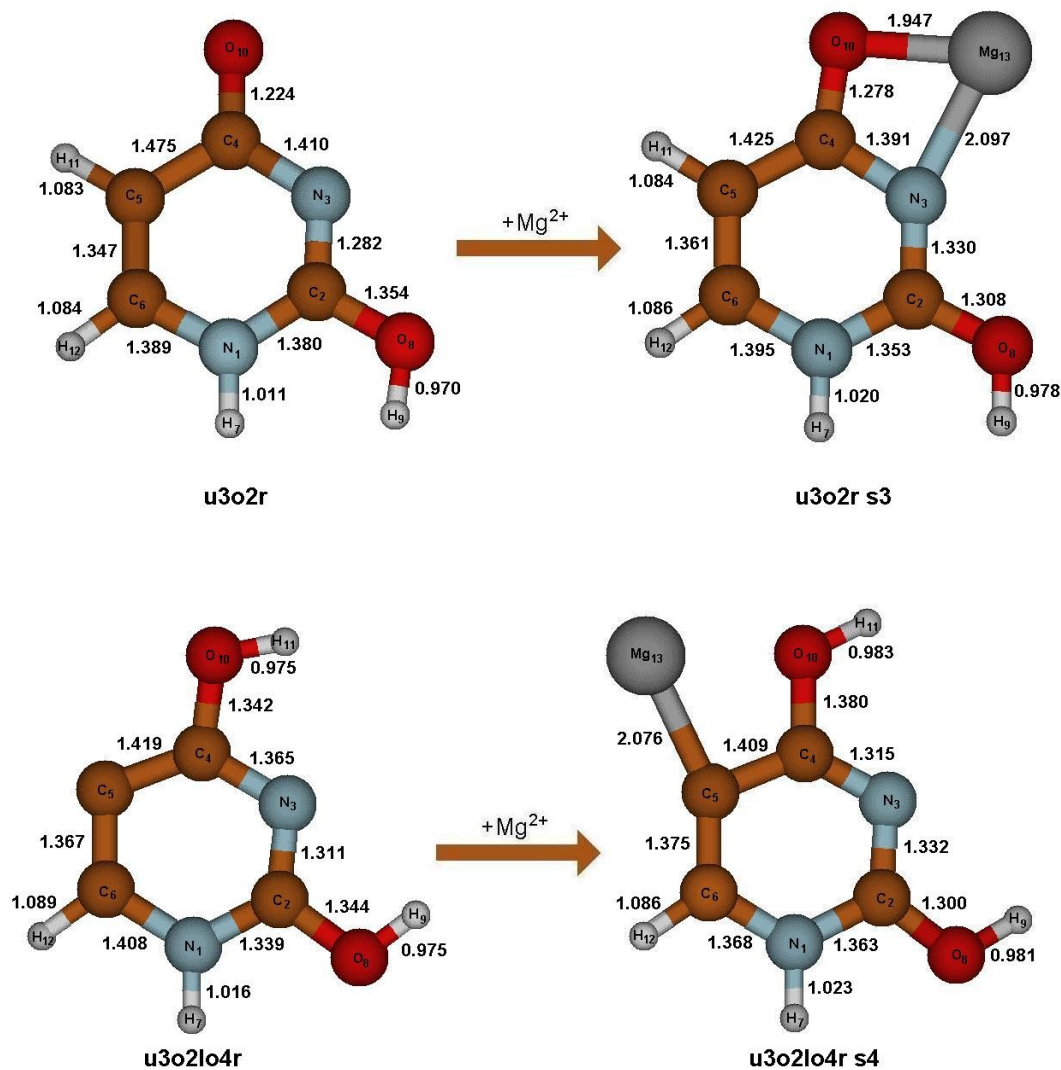


**Fig. 20** Changes of bond distances upon  $Mg^{2+}$  binding in case of uracil tautomer. As „O8“ is denoted O2 oxygen, and „O10“ oxygen represents O4 oxygen.

Magnesium ion causes deformation of uracil bonds as a mechanism of stabilisation (see Table 11 and Figure 20). These changes depends on the position of the magnesium ion and on the keto/enol tautomerism.

If the magnesium is located on the first binding site S1, then the magnesium binds to oxygen O2 and nitrogen N1 in a bidentate manner that has a strong stabilizing effect. In all cases the bond C2-O2 is lengthened. For u1o4r\_s1 the prolongation is 0.058 Å with respect to its tautomer without magnesium ion. For uo2lo4r\_s1 it is equal to 0.054 Å and for uo2lo4r\_s1 it is about 0.057 Å (see Table 11). Bonds N3-C4, C4-C5 and C6-N1 are lengthened, too. On the other hand bonds C2-N3, C5-C6 and C4-O10 are

shortened. Bond N1-C2 is shortened only for the N-Mg-O binding motif while for the N-Mg-O2H binding motif it is lengthened. See u1o4r → u1o4r\_s1 in Figure 20.

Magnesium ion located on site S1/S2 induces prolongation of the bond C2-O2. In the structure u1\_s1/s2 the magnesium ion binds by a monodentate manner to O2 atom and the bond N1-C2 is shortened. The other bonds have similar behaviour as in the case of magnesium bidentate binding on site S1.

In the position S2 magnesium binds to oxygen O2 and nitrogen N3 in a bidentate manner. The bond C2-O2 is always lengthened and bond N1-C2 is markedly shortened. The change of bond C2-N3 depends on the kind of the tautomer, concretely on the keto/enol character of the O2 atom. The N3-Mg-O2H binding motif induces prolongation of the bond C2-N3 because Mg<sup>2+</sup>...H interaction is not feasible, whereas the N3-Mg-O2 binding motif causes its shortening. The same results were obtained for bond C4-C5, the reverse results for bond C5-C6. Bond N3-C4 is lengthened for all tautomers and bond C4-O10 is shortened. See u3o4l → u3o4l\_s2 transition in Figure 20.

Magnesium located in position S3 causes similar effects as in position S1. Bonds C2-O2, N1-C2, C4-C5 are shortened, while bonds C5-C6 and C4-O4 are lengthened. The bond C2-N3 is generally lengthened, only in case of u3o2l\_s3 it is shortened. For keto-enol tautomers, where O4 atom represents keto group, bond N3-C4 is shortened, whereas the other are lengthened. Bond C6-N1 are shortened only in case of u3o2r\_s3. See u3o2r → u3o2r\_s3 transition in Figure 20.

Deformation effects on the pyrimidine ring caused by magnesium ion binding on the site S3/S4 are shown in Figure 20 for u1 → u1\_s3/s4 transition, for magnesium ion binding on the site S4 they are shown for u3o2lo4r → u3o2lo4r\_s4 transition. In all cases bonds C2-O8, N3-C4, C4-C5 and C6-N1 are shortened, while bonds C4-O10, N1-C2, C2-N3 and C5-C6 are lengthened.

Magnesium ion causes deformation of uracil bonds as a mechanism of stabilisation (see Table 11 and Figure 20). These changes depends on the position of the magnesium ion and on the keto/enol tautomerism.

If the magnesium is located on the first binding site S1, then the magnesium binds to oxygen O2 and nitrogen N1 in a bidentate manner that has a strong stabilizing effect. In all cases the bond C2-O2 is lengthened. For u1o4r\_s1 the prolongation is 0.058 Å with respect to its tautomer without magnesium ion. For uo2lo4r\_s1 it is equal to 0.054 Å and for uo2lo4r s1 it is about 0.057 Å (see Table 11). Bonds N3-C4, C4-C5 and C6-N1 are lengthened, too. On the other hand bonds C2-N3, C5-C6 and C4-O10 are shortened. Bond N1-C2 is shortened only for the N-Mg-O binding motif while for the N-Mg-O2H binding motif it is lengthened. See u1o4r → u1o4r\_s1 in Figure 20.

Magnesium ion located on site S1/S2 induces prolongation of the bond C2-O2. In the structure u1\_s1/s2 the magnesium ion binds by an monodentate manner to O2 atom and the bond N1-C2 is shortened. The other bonds have similar behaviour as in the case of magnesium bidentate binding on site S1.

In the position S2 magnesium binds to oxygen O2 and nitrogen N3 in a bidentate manner. The bond C2-O2 is always lengthened and bond N1-C2 is markedly shortened. The change of bond C2-N3 depends on the kind of the tautomer, concretely on the keto/enol character of the O2 atom. The N3-Mg-O2H binding motif induces prolongation of the bond C2-N3 because Mg<sup>2+</sup>...H interaction is not feasible, whereas the N3-Mg-O2 binding motif causes its shortening. The same results were obtained for bond C4-C5, the reverse results for bond C5-C6. Bond N3-C4 is lengthened for all tautomers and bond C4-O10 is shortened. See u3o4l → u3o4l\_s2 transition in Figure 20.

Magnesium located in position S3 causes similar effects as in position S1. Bonds C2-O2, N1-C2, C4-C5 are shortened, while bonds C5-C6 and C4-O4 are lengthened. The bond C2-N3 is generally lengthened, only in case of u3o2l\_s3 it is shortened.. For keto-enol tautomers, where O4 atom represents keto group, bond N3-C4 is shortened, whereas the other are lengthened. Bond C6-N1 are shortened only in case of u3o2r\_s3. See u3o2r → u3o2r\_s3 transition in Figure 20.

Deformation effects on the pyrimidine ring caused by magnesium ion binding on

the site S3/S4 are shown in Figure 20 for  $u1 \rightarrow u1\_s3/s4$  transition, for magnesium ion binding on the site S4 they are shown for  $u3o2lo4r \rightarrow u3o2lo4r\_s4$  transition. In all cases bonds C2-O8, N3-C4, C4-C5 and C6-N1 are shortened, while bonds C4-O10, N1-C2, C2-N3 and C5-C6 are lengthened.

### 3.3 The Comparison of $Mg^{2+}$ binding to the most stable Tautomers of Thymine and Uracil

Thymine is known as 5-methyluracil, it is a pyrimidine base in the nucleic acid of DNA. Thymine is replaced by uracil in RNA. We made an effort to examine energetic differences between uracil and thymine tautomers that are derived by methylation of uracil at the carbon C5, see Figure 21. We compared energies of the sixty-five most stable uracil tautomers with their thymine counterparts adopting B3LYP and MP2 methods using standard G03 parameters. Our results for the  $Mg^{2+}$  binding to thymine were compared with the results of Kabeláč and Hobza.<sup>35</sup> They investigated the stabilisation energies of  $Mg^{2+}$  binding to thymine tautomers using an approximate resolution of identity MP2 (RI-MP2) method with Ahlich's TZVPP ([5s3p3d1f/3s2p1d]) basis set using TURBOMOLE 5.6 program suite. Some uracil tautomers does not have thymine counterparts, see Figure 22. All energetical calculations were done in the gas-phase environment.

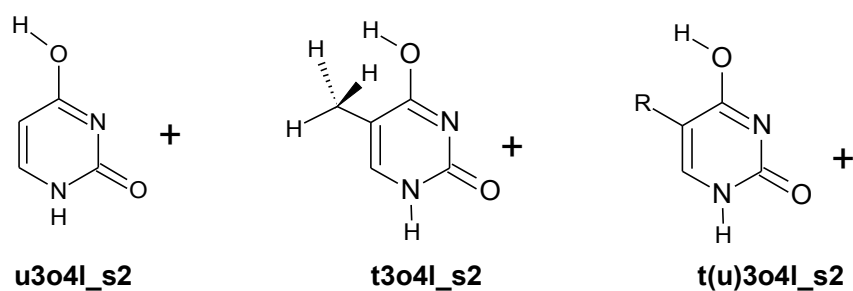


**Fig. 21** Schematic drawing of uracil tautomer and its thymine counterparts. The third schematic drawing will be used thereafter.

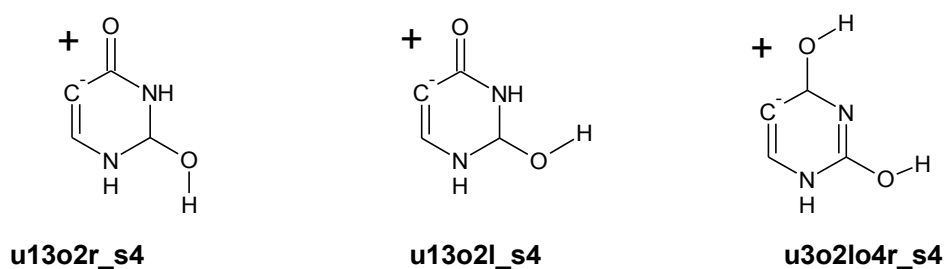
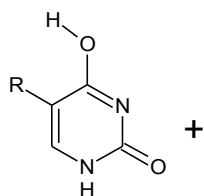
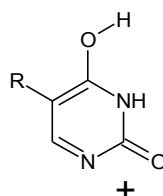


**Fig. 22** Schematic drawings of uracil tautomers that does not have its thymine counterparts.



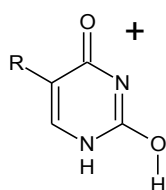
t(u)3o4l  
+17.5/18.5/+17.1

t(u)3o4l\_s2 -171.0/-176.5/-174.4



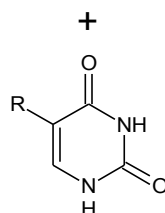
t(u)1o4r  
+23.6/+25.6/+24.2

t(u)1o4r\_s1 -169.7/-176.5/-173.9



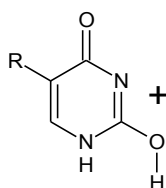
t(u)3o2r  
+27.8/+26.9/+27.4

t(u)3o2r\_s3 -176.5/-180.8/-179.5



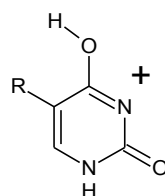
t(u)1  
+0.0/+0.0/+0.0

t(u)1\_s3/s4 -130.5/-134.0/-130.4



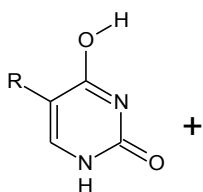
t(u)3o2r  
+27.8/+26.9/+27.4

t(u)3o2r\_s2 -170.5/-c/-150.3



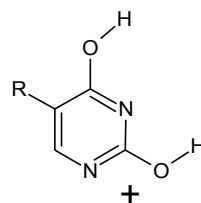
t(u)3o4l  
+17.5/+18.5/+17.1

t(u)3o4l\_s3 -146.0/-150.2/-151.5



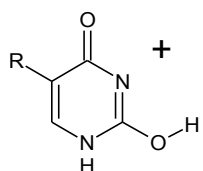
t(u)3o4r  
+10.8/+11.6/+10.2

t(u)3o4r\_s2 -158.4/-164.0/-161.6



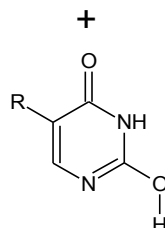
t(u)o2lo4r  
+10.6/+10.9/+9.4

t(u)o2lo4r\_s1 -141.2/-145.0/-152.5



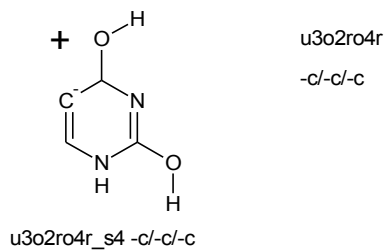
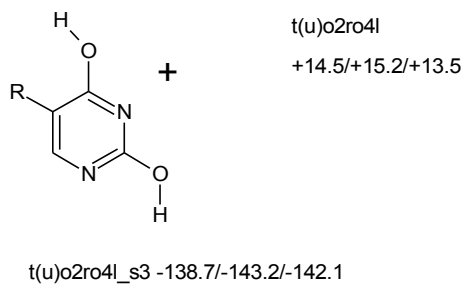
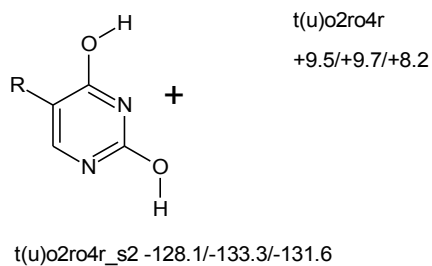
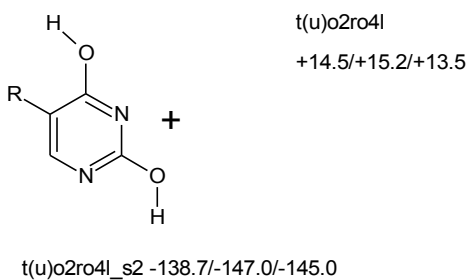
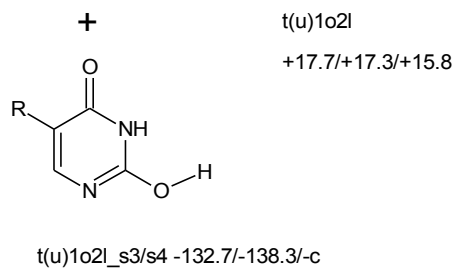
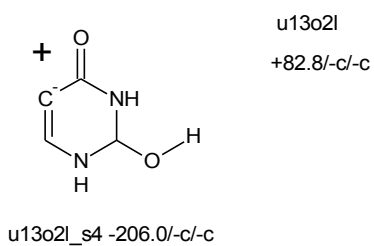
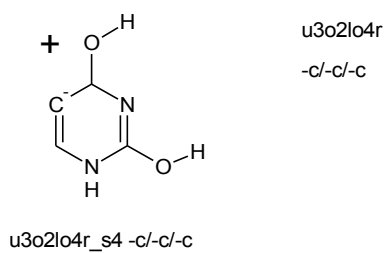
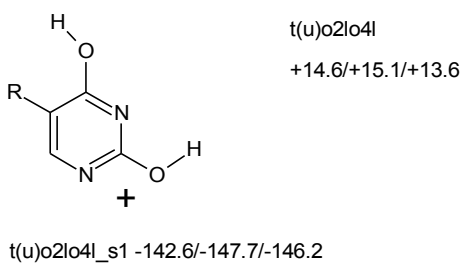
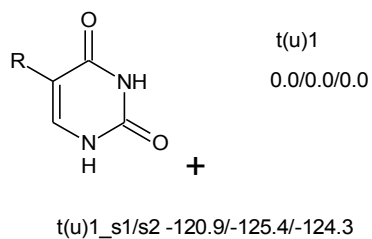
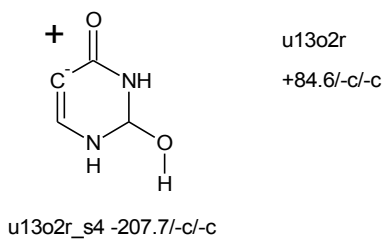
t(u)3o2l  
+17.7/+17.0/+15.5

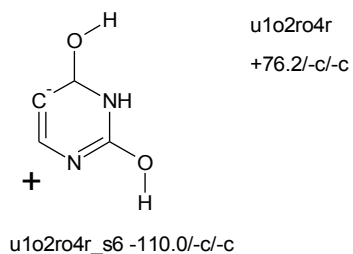
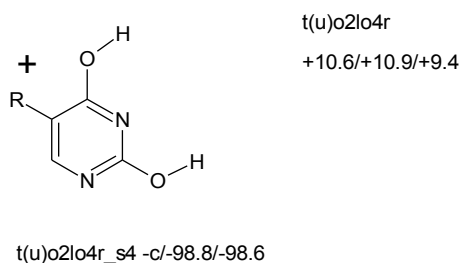
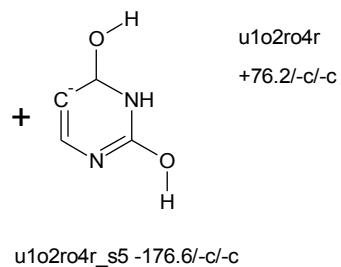
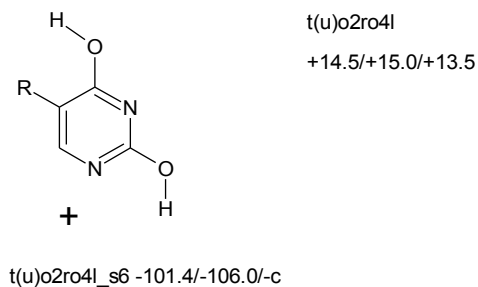
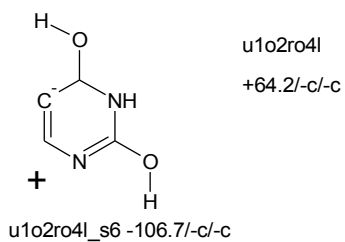
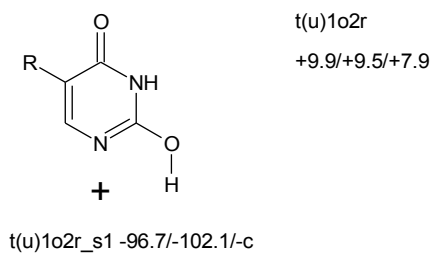
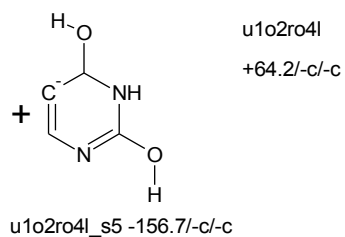
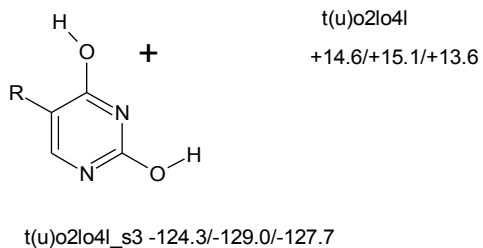
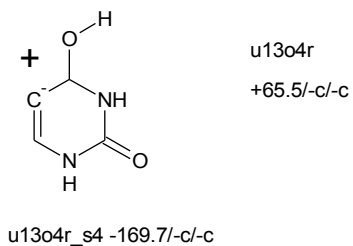
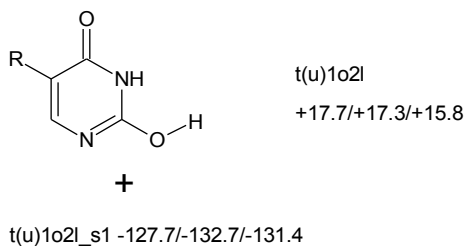
t(u)3o2l\_s3 -165.5/-171.0/-166.7

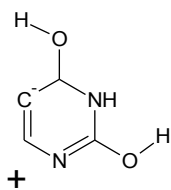


t(u)1o2r  
9.9/+9.5/+7.9

t(u)1o2r\_s4 -135.7/-140.5/-136.5

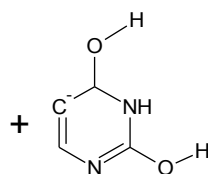






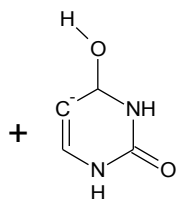
u1o2lo4l  
+72.8/-c/-c

u1o2lo4l\_s6 -126.7/-c/-c



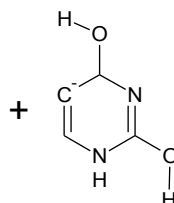
u1o2lo4r  
+86.5/-c/-c

u1o2lo4r\_s5 -176.0/-c/-c



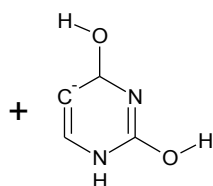
u13o4l  
+53.4/-c/-c

u13o4l\_s5 -147.0/-c/-c



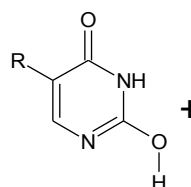
u3o2ro4l  
+69.8/-c/-c

u3o2ro4l\_s5 -155.2/-c/-c



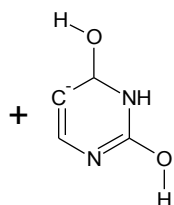
u3o2lo4l  
+61.1/-c/-c

u3o2lo4l\_s5 -155.4/-c/-c



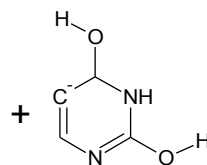
t(u)1o2r  
+9.9/+9.5/+7.9

t(u)1o2r\_s2 -c/-68.0/-101.0



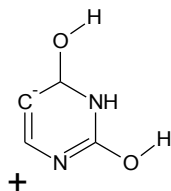
u3o2ro4l  
+69.8/-c/-c

u3o2ro4l\_s5 -155.2/-c/-c



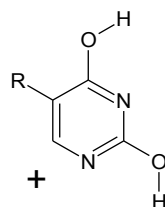
u1o2lo4l  
+72.9/-c/-c

u1o2lo4l\_s5 -156.9/-c/-c



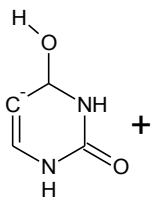
u1o2lo4r  
+86.5/-c/-c

u1o2lo4r\_s6 -126.5/-c/-c



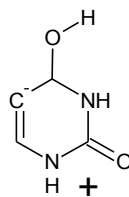
t(u)o2ro4r  
+9.5/+9.7/+8.2

t(u)o2ro4r\_s6 -101.6/-106.7/-c



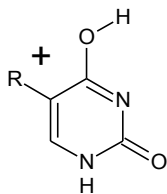
u13o4l  
+53.4/-c/-c

u13o4l\_s2 -117.4/-c/-c



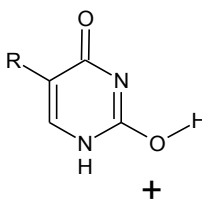
u13o4r  
+65.5/-c/-c

u13o4r\_s1 -113.8/-c/-c



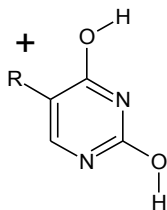
t(u)3o4r  
+10.8/+11.6/+10.2

t(u)3o4r\_s4 -98.0/-96.6/-145.2



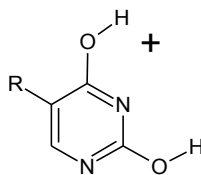
t(u)3o2l  
+17.6/+16.96/+15.5

t(u)3o2l\_s1 -63.9/-90.6/-87.7



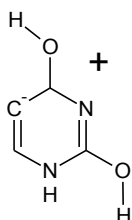
t(u)o2ro4r  
+9.5/+9.7/+8.2

t(u)o2ro4r\_s4 -94.3/-100.4/-95.3



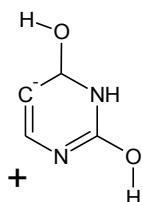
t(u)o2lo4r  
+10.6/+10.9/+9.4

t(u)o2lo4r\_s3 -75.6/-80.6/-c



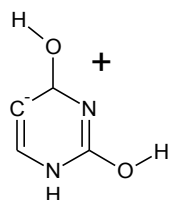
u3o2ro4l  
+69,8/-c/-c

u3o2ro4l\_s3 -144.7/-c/-c



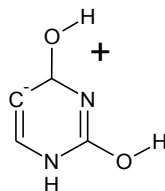
u1o2ro4l  
+64.2/-c/-c

u1o2ro4l\_s6 -106.7/-c/-c



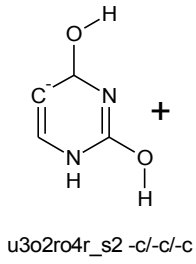
u3o2lo4l  
+61,1/-c/-c

u3o2lo4l\_s3 -131.9/-c/-c

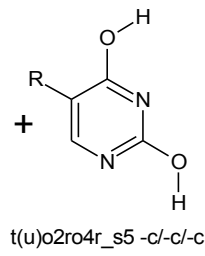


u3o2lo4r  
+c/-c/-c

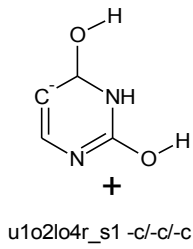
u3o2lo4r\_s3 -c/-c/-c



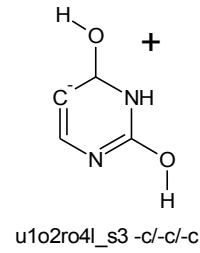
u3o2ro4r  
-c/-c/-c



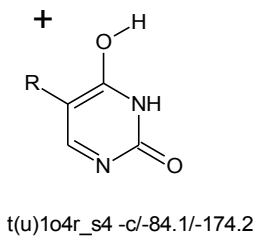
t(u)o2ro4r  
+9.5/+9.72/+8.2



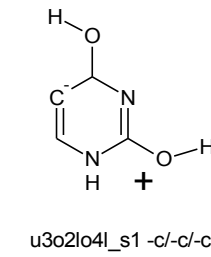
u1o2lo4r  
-86.5/-c/-c



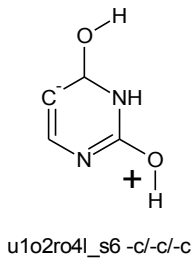
u1o2ro4l  
+64.2/-c/-c



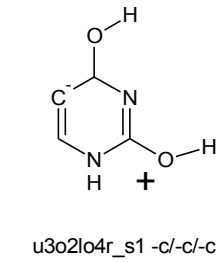
t(u)1o4r  
+23.6/+25.6/+24.2



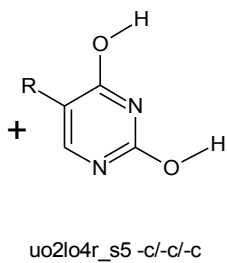
u3o2lo4l  
+61.1/-c/-c



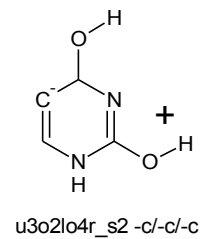
u1o2ro4l  
+64.2/-c/-c



u3o2lo4r  
-c/-c/-c



uo2lo4r  
+10.6/+10.9/+9.4



u3o2lo4r  
-c/-c/-c

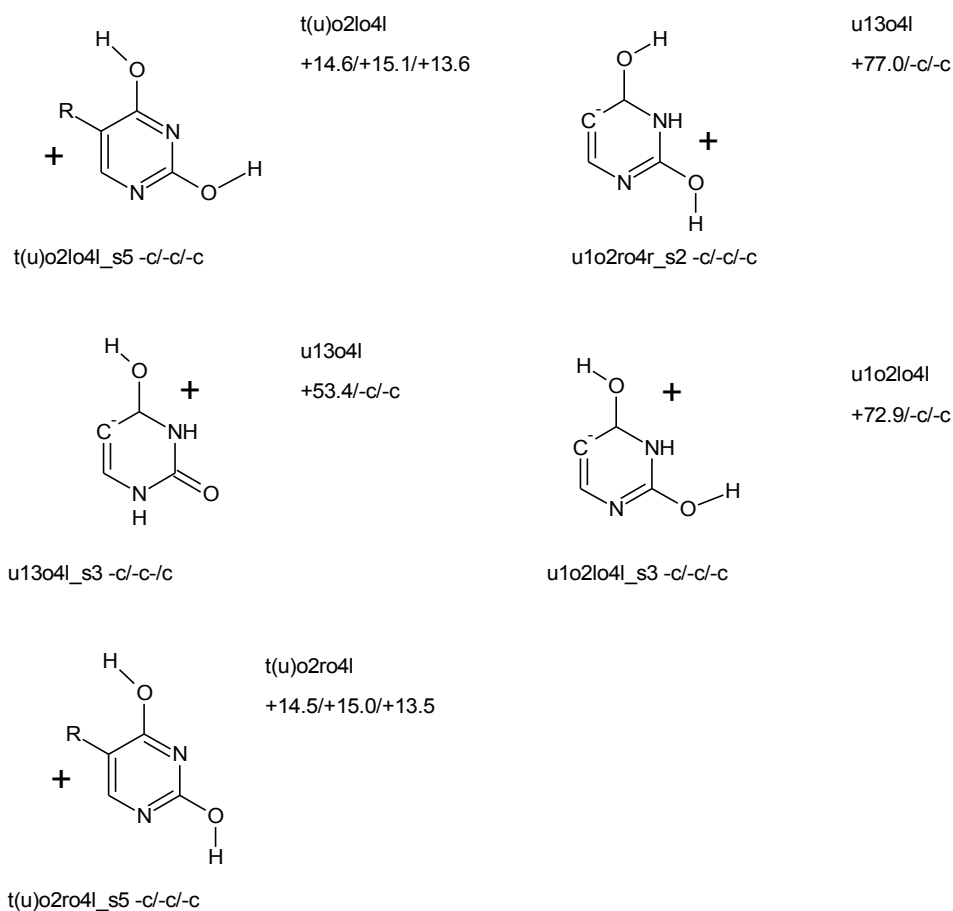


**Fig. 23** Schematic drawings of the optimized structures of metalated thymine and uracil. The stabilisation energies (in kcal/mol at MP2/6-311++G(2df,2pd)//B3LYP-6-311++G\*\* level of theory) are shown for uracil, thymine and for thymine according to work of Kabeláč and Hobza<sup>35</sup> in this order. A letter "c" means that the energy could not be calculated for one of the following reasons: 1) the thymine tautomer does not exist, 2) the geometry of tautomer was changed during the optimisation or 3) magnesium ion moved to more feasible site (see Figure 17). The relative stability of the structures in respect to the canonical form is written at the right edge of the schematic drawing (See Tables 9, 12, 17).

**Table 12: Gas phase energies for thymine ... Mg<sup>2+</sup> complexes**

Structure	E <sub>comp</sub>	E <sub>Udef</sub>	E <sub>Uned</sub>	BSSE	E <sub>Def</sub>	E <sub>int</sub>	E <sub>rel-comp</sub>	E <sub>rel-taut</sub>
t1_s4	-652.347738	-453.291080	-453.308468	1.68	10.91	-134.03	23.96	0.00
t1_s1/s2	-652.333330	-453.293738	-453.308468	1.31	9.24	-125.36	32.63	0.00
t1o2l_s1	-652.318561	-453.266805	-453.280952	1.82	8.88	-132.69	42.56	17.27
t1o2l_s4	-652.327381	-453.263321	-453.280952	1.77	11.06	-138.28	36.97	17.27
t1o2r_s4	-652.342997	-453.275341	-453.293359	1.73	11.31	-140.49	26.98	9.48
t1o2r_s1	-652.281241	-453.281362	-453.293359	1.22	7.53	-102.10	65.37	9.48
t1o2r_s2	-652.226471	-453.281297	-453.293359	1.00	7.57	-67.98	99.48	9.48
t1o4l_s1	-c	-c	-453.272993	-c	-c	-c	-c	22.26
t1o4l_s3	-c	-c	-453.272993	-c	-c	-c	-c	22.26
t1o4r_s1	-652.375163	-453.253671	-453.267672	2.07	8.79	-176.46	7.13	25.60
t1o4r_s4	-652.227412	-453.250681	-453.267672	1.57	10.66	-84.08	99.51	25.60
t3o2l_s3	-652.377259	-453.266588	-453.278665	1.97	7.58	-170.97	5.72	18.70
t3o2l_s1/s2	-652.248734	-453.236682	-453.278665	1.71	26.35	-90.58	86.11	18.70
t3o2r_s3	-652.380175	-453.253093	-453.265557	2.06	7.82	-180.79	4.13	26.93
t3o2r_s2	-c	-c	-453.265557	-c	-c	-c	-c	26.93
t3o4l_s2	-652.386866	-453.265905	-453.278927	2.13	8.17	-176.53	0.00	18.54
t3o4l_s3	-652.344465	-453.267737	-453.278927	1.85	7.02	-150.19	26.33	18.54
t3o4r_s2	-652.377763	-453.276029	-453.289974	2.07	8.75	-163.94	5.66	11.61
t3o4r_s4	-652.272794	-453.272007	-453.289974	1.58	11.27	-98.56	71.04	11.61
to2lo4l_s1	-652.345805	-453.272618	-453.284365	1.83	7.37	-147.65	25.47	15.13
to2lo4l_s3	-652.316107	-453.270156	-453.284365	1.82	8.92	-129.01	44.10	15.13
to2lo4r_s1	-652.351266	-453.276921	-453.291128	1.83	8.91	-146.98	21.89	10.88
to2lo4r_s2/s3	-652.244568	-453.270537	-453.291128	1.29	12.92	-80.57	88.30	10.88
to2lo4r_s4	-652.274122	-453.271071	-453.291128	1.61	12.59	-98.79	70.08	10.88
to2ro4l_s2	-652.344811	-453.273875	-453.284534	1.86	6.69	-146.88	26.12	15.02
to2ro4l_s3	-652.338814	-453.272649	-453.284534	1.82	7.46	-143.16	29.85	15.02
to2ro4l_s6	-652.278632	-453.269655	-453.284534	1.21	9.34	-106.02	66.99	15.02
to2ro4r_s2	-652.331535	-453.280542	-453.292972	1.85	7.80	-133.27	34.45	9.72
to2ro4r_s6	-652.288234	-453.278777	-453.292972	1.22	8.91	-106.74	60.97	9.72
to2ro4r_s4	-652.278806	-453.275014	-453.292972	1.61	11.27	-100.41	67.30	9.72

Energies of the thymine tautomers were calculated at MP2/6-311++G(2df,2pd)//B3LYP-6-311++G\*\* level of theory. . See Table 9 for the description of the terms. The relative stability of the complex with respect to the canonical form is shown in the eighth column( $E_{rel-comp}$ ). The last column shows relative stability of the tautomers with respect to the canonical form( $E_{rel-taut}$ ).

### 3.4 Binding of Hydrated Magnesium Ion to Uracil Tautomers

In water environment magnesium ion is surrounded by water ligands. These ligands can be exchanged for electronegative groups of biomolecules if it is energetically feasible. The ligands form usually an octahedral arrangement around Mg<sup>2+</sup> ion. In our study we focused on the pentahydrated and hexahydrated magnesium in the

vicinity of two selected uracil tautomers. The first one is the canonical structure u1 - the most stable tautomer in the gas phase on which magnesium cation binds via O4 atom. A structure similar to u1\_s3/s4 was studied but this time  $Mg^{2+}$  ion was hydrated. The second tautomer is u3o4l enol-keto tautomer which enables the bidentate binding of  $Mg^{2+}$  ion to O2 and N3 centers forming the most stable complex of uracil with the bare  $Mg^{2+}$  ion (see Tables 10 and 11).

We considered the following sequence of events: at first the hexahydrated magnesium interacted with uracil only by hydrogen bonds via coordinated water ligands (an absorption step), then one water ligand was pushed away into the second coordination shell and the keto oxygen was coordinated to  $Mg^{2+}$  ion instead (the first binding step). For the u3o4l enol-keto tautomer the third step was also considered to enable the bidentate binding with N3 and O2 atoms (the second binding step).

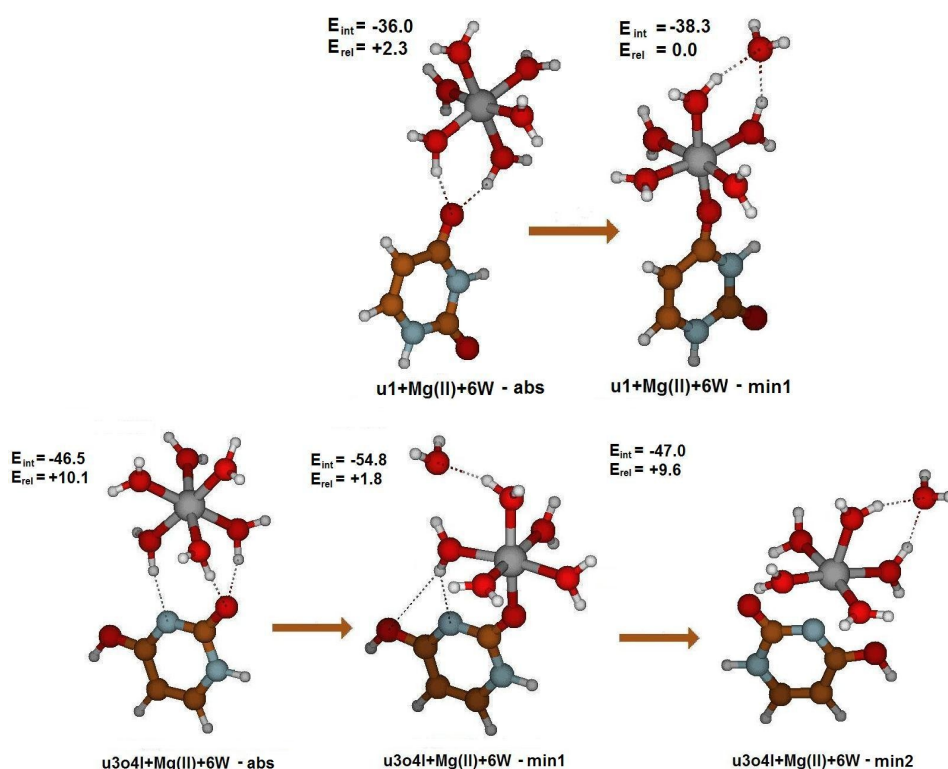


**Fig. 24** Binding of  $Mg(H_2O)_6^{2+}$  ion to uracil. The most stable di-keto and keto-enol tautomers are considered (see text). Relative energies with respect to the most stable u3o4l-min1 complex are shown for the absorbed and bound (the first and second minimum) structures.

We investigated the total energies of the absorbed structures, the first minimum and the second minimum (only for u3o4l tautomer) structures. We calculated relative energies between these structures and compared them with the relative energies of u1 and u3o4l tautomers and with relative energies of u1\_s3/s4 and u3o4l\_s2 complexes. A similar comparison was made also for interaction energies. The same procedure was carried out in the case of the thymine system (see Tables 10, 11, 12, 13, 16 and Figure 24).

**Table 13: The comparison of uracil tautomers with bound hydrated magnesium ions**

Tautomer	The electronic energy		The correction	The Gibbs free energy	
	HF/3-21+G*	B3LYP/6-31+G*	$\Delta G$	HF/3-21+G*	B3LYP/6-31+G*
u1+Mg(II)+6W-abs	-1062.344711	-1073.183423	0.185431	-1062.159280	-1072.997992
u1+Mg(II)+6W-min1	-1062.352998	-1073.187625	0.184440	-1062.168558	-1073.003185
u3o4l+Mg(II)+6W-abs	-1062.338131	-1073.186186	0.189384	-1062.148747	-1072.996802
u3o4l+Mg(II)+6W-min1	-1062.344721	-1073.189010	0.185688	-1062.159033	-1073.003322
u3o4l+Mg(II)+6W-min2	-1062.336172	-1073.178425	0.188816	-1062.147356	-1072.989609

The comparison of microhydrated magnesium cation in the vicinity of the most stable di-keto form and keto-enol form of uracil tautomers. The first describes the name of the structure (abs - the absorbed structure, min1 - the first minimum, min2 - the second minimum). The second and third columns show the electronic energies of the system on HF and B3LYP levels. The fourth column summarizes the thermal correction of the Gibbs free energy (calculated at B3LYP/6-31+G\* level). The last columns contain the informations about corrected energies of the system. The values are in Hartree units.

**Table 14: The comparison of thymine tautomers with bound hydrated magnesium ions**

Tautomer	The electronic energy		The correction	The Gibbs free energy	
	HF/3-21+G*	B3LYP/6-31+G*	$\Delta G$	HF/3-21+G*	B3LYP/6-31+G*
t1+Mg(II)+6W-abs	-1101.170883	-1112.503073	0.213061	-1100.957822	-1112.290012
t1+Mg(II)+6W-min1	-1101.177055	-1112.506825	0.211784	-1100.965271	-1112.295041
t3o4l+Mg(II)+6W-abs	-1101.156370	-1112.497015	0.212359	-1100.944011	-1112.284656
t3o4l+Mg(II)+6W-min1	-1101.173851	-1112.512758	0.212326	-1100.961525	-1112.300432
t3o4l+Mg(II)+6W-min2	-1101.164729	-1112.501839	0.215019	-1100.949710	-1112.286820

The comparison of microhydrated magnesium cation in the vicinity of the most stable di-keto form and keto-enol form of thymine tautomers. See Table 13 for the description of the terms..

**Table 15: The interaction energies of uracil tautomers with bound hydrated magnesium cation**

Structure	$E_{comp}$	$E_{Udef}$	$E_{UMg+6W}$	$E_{Unsd}$	$E_{rel-taut}$	BSSE	$E_{Def}$	$E_{def(Mg+6W)}$	$E_{int}$	$E_{tot}$	$E_{rel-comp}$
u1+Mg(II)+6W-abs	-1073.559696	-414.967077	-658.516156	-414.972366	0.00	0.65	3.32	8.00	-36.01	-36.01	2.28
u1+Mg(II)+6W-min1	-1073.564019	-414.966905	-658.505739	-414.972366	0.00	1.08	3.43	14.54	-38.29	-38.29	0.00
u3o4l+Mg(II)+6W-abs	-1073.547488	-414.930799	-658.513741	-414.943205	18.30	0.81	7.78	9.52	-46.48	-28.19	10.11
u3o4l+Mg(II)+6W-min1	-1073.561405	-414.931227	-658.500679	-414.943205	18.30	1.24	7.52	17.71	-54.79	-36.49	1.80
u3o4l+Mg(II)+6W-min2	-1073.549427	-414.933817	-658.498443	-414.943205	18.30	1.53	5.89	19.12	-46.99	-28.69	9.61

Interaction energies of microhydrated magnesium cation in the vicinity of the most stable di-keto and keto-enol form of uracil tautomers. The interaction energies contain the deformation energies of uracil tautomers and the deformation energies of hydrated magnesium. See Tables 9, 12 and 13 for the description of the terms.. The fourth column is represented by energy of hydrated magnesium in this system ( $E_{UMg+6W}$ ). The ninth column summarizes the deformation energies of hexahydrated magnesium. The next to the last column shows the total energy of the system ( $E_{tot}$ ). The total energy of the hexahydrated magnesium cation is -658,528909 a.u.

**Table 16: The interaction energies of thymine tautomers with bound hydrated magnesium cation**

Name	$E_{\text{comp}}$	$E_{\text{Udef}}$	$E_{\text{UMe+6W}}$	$E_{\text{Ured}}$	$E_{\text{rel-taut}}$	BSSE	$E_{\text{Def}}$	$E_{\text{def(Mg+6W)}}$	$E_{\text{int}}$	$E_{\text{int}}$	$E_{\text{rel-comp}}$
t1+Mg(II)+6W-abs	-1112.891449	-454.299306	-658.515370	-454.304706	0.00	0.77	3.39	8.50	-35.53	-35.53	7.07
t1+Mg(II)+6W-min1	-1112.894238	-454.299342	-658.504008	-454.304706	0.00	1.11	3.37	15.63	-36.93	-36.93	5.67
t3o4l+Mg(II)+6W-abs	-1112.888438	-454.266840	-658.513749	-454.273390	19.65	0.81	4.11	9.51	-53.24	-33.59	9.01
t3o4l+Mg(II)+6W-min1	-1112.903458	-454.267232	-658.500677	-454.273390	19.65	1.23	3.86	17.72	-62.25	-42.60	0.00
t3o4l+Mg(II)+6W-min2	-1112.891310	-454.269633	-658.498455	-454.273390	19.65	1.53	2.36	19.11	-54.33	-34.68	7.92

*Interaction energies of microhydrated magnesium cation in the vicinity of the most stable di-keto and keto-enol form of thymine tautomers. See Tables 9, 12, 13 and 15 for the description of the terms..*

Our results show that gas-phase data are not transferable to the solution since just the first water coordination shell fully diminishes the energy gap between the most stable u3o4l\_2s structure (the rare enol-keto tautomer stabilized by the metal ion) and the canonical u1\_s3/s4 structure (see Tables 13 and 15). Similar results were obtained for t3u4l\_2s and t1\_s3/s4 tautomers of thymine (see Tables 14 and 16). Clearly the environment has the protective and shielding effects against the possible shifts of tautomeric equilibria caused by metal ions. It is in agreement with a recent study of Kosenkov et al.<sup>52</sup>. Note that most studies deal with the interactions between the nucleobase and the bare metal ion.<sup>9, 35, 53-55</sup>

Our future work will be focused on the evaluation of the influence of the phosphate group in the metal's first coordination shell on the relative energies since phosphates are the primary targets of Mg<sup>2+</sup> binding to nucleic acids. The effect of bulk water molecules will be also shown.

## 4 Conclusions

We used DFT and MP2 calculations to investigate the tautomeric forms of uracil and their interactions with bare and hydrated magnesium cation in the gas phase. The results were compared with tautomeric forms of thymine and it turned out that the uracil has very similar properties as the thymine tautomers. Below we summarize the results only for the uracil, but the same conclusions apply to thymine.

The most feasible interactions of bare magnesium with uracil is in a bidentate manner. It leads to the stabilization of the enol tautomers. The most stable metalated uracil tautomer is denoted as u3o4l\_s2, interaction energy between the metal and u3o4l tautomer is - 171.0 kcal/mol. On the other hand structure u1\_s3/s4 is destabilized by 22.3 kcal/mol with respect to u3o4l\_s2, despite the fact that di-keto tautomer u1 is the most stable tautomer of the bare uracil and u3o4l is by 16.8 kcal/mol less stable. The magnesium binds to oxygen O4 in a monodentate manner and it is a reason of a decreased stability of u1\_s3/s4 since bidentate binding has a stronger stabilizing effect. Interaction energy between u1 tautomer and the metal is only - 130.5 kcal/mol. The five most stable uracil ... Mg<sup>2+</sup> structures are metal complexes with rare tautomers (see Tables 7 and 8).

We have studied the changes of bond distances upon Mg<sup>2+</sup> binding in case of uracil tautomer. Magnesium ion causes deformation of bonds of uracil tautomers as a result of a strong polarization effect. Some bonds are shortened, while other bonds are lengthened. That is why we can not neglect the deformation energies when calculating interaction energies.

The water environment cancels out the Mg<sup>2+</sup> preference of the bidentate binding. In fact the monodentate binding of hydrated Mg<sup>2+</sup> is preferred even in the u3o4l being by 7.8 kcal/mol more stable than the bidentate binding. The most stable complex is u1+Mg(II)+6w-min1 complex being by 1.8 kcal/mol more stable than u3o4l+Mg(II)+6w-min1. The higher stability of u1 tautomer is still almost compensated by the presence of a strong N3...H<sub>2</sub>O H-bond in the second structure.

## References

1. Greenwood N. N., Earnshaw A., *Chemie prvku - svazek1*, Informatorium **1993** (in Czech)
2. Kluge S., Weston J. *Biochemistry* **2005**, 44, 4877
3. Bandyopadhyay D., Bhattacharyya D., *J. Biomol. Struct. Dyn.* **2003**, Vol. 21, No. 3, ISSN 0739-1102
4. Atkins P. W., *Shiver & Atkins inorganic chemistry*, Oxford **2006**
5. Reginald H. Garrett, Charles M. Grisham, *Biochemistry*, Harcourt College Pub; Package edition **1996**
6. Tsai C. Stan, *Biomacromolecules: Introduction to structure, function and informatics*, Hoboken, NJ: Wiley – Liss, **2007**
7. Xingbang Hu, Haoran Li, Lei Zhang, Shijun Han, *J. Phys. Chem. B*, **2007**, 111, 9347-9354
8. Kabeláč M., Hobza P., *Phys. Chem. Chem. Phys.*, **2007**, 9, 903-917
9. Rincón E., Yáñez M., Toro-Labbé A., MÓ O., *Phys. Chem. Chem. Phys.*, **2007**, 9, 2531-2537
10. Rincón E., Jaque P., Toro-Labbé A., *J. Phys. Chem. A*, **2006**, 110, 9478-9485
11. Wu R., McMahon T. B., *J. Am. Chem. Soc.*, **2007**, 129, 569-580
12. Drapper D. E., *RNA*, **2004**, 10, 335-343
13. Bertini I.: *Biological inorganic chemistry: structure and reactivity*. Kausalito: University Science Books, **2007**
14. Martick M., Scott W. G., *Cell* **2006**, 126, 309-320
15. Torres R. A., Himo F., Bruice T. C., Noodleman L., Lovell T., *J. Am. Chem. Soc.* **2003**, 125, 9861
16. Leclerc F., Karplus M., *J. Phys. Chem. B* **2006**, 110, 3395
17. Lee T. S., Silva Lopez C., Giambasu G. M., Martick M., Scott W. G., York, D.M. *J. Am. Chem. Soc.* **2008**, 130, 3053

18. Martick M., Scott W.G., *Cell* **2006**, 126, 309
19. Cochrane J. C., Strobel S. A., *Acc. Chem. Res.* **2008**, Vol. 41, No. 8, 1027-1035
20. Takagi Y., Warashina M., Stec W. J., Yoshinari K., Taira K., *Nucleic Acids Res.* **2001**, Vol. 29, No. 9, 1815-1834
21. Freisinger E., Sigel R. K. O., *Coord. Chem. Rev.* **2007**, 251, 1834-1851
22. Rueda M., Kalko S. G., Luque F. J., Orozco M., *J. Am. Chem. Soc.* **2003**, 125, 8007
23. Hemat R.A.S., Water, Urotext, ISBN 1903737125, 9781903737125
24. Palafox M.A., Iza N., de la Fuente M., Navarro R.J. *Phys. Chem. B* **2009**, 113, 2458
25. Schneider B., Berman H.M., *Biophys. J.* **1995**, 69, 2661
26. Arai S., Chatake T., Ohhara T., Kuruhara K., Tanaka I., Suzuki N., Fujimoto Z., Mizuno H., Niimura N., *Nucleic Acids Res.* **2005**, 33, 3017
27. Gu B., Zhang F. S., Wang Z. P., Zhou H.Y., *Phys. Rev. Lett.* **2008**, 100, 088104
28. Neidle, Stephen. *Nucleic Acid Structure and Recognition*, Oxford University Press, 2002, p. 97.
29. Rejnek J., Hanus M., Kabeláč M., Ryjáček F., Hobza P., *Phys. Chem. Chem. Phys.*, **2005**, 7, 2006-2017
30. Trygubenko S. A., Bogdan T. V., Rueda M., Orozco M., Luque F.J., Šponer J., Slavíček P., Hobza P., *Phys. Chem. Chem. Phys.* **2002**, 4, 4192
31. Hanus M., Ryjáček F., Kabeláč M., Kubař T., Bogdan T. V., Trygubenko S. A., Hobza P., *J. Am. Chem. Soc.* **2003**, 125, 7678-7688
32. Marino T., Mazzuca D., Toscano M., Russo N., Grand A., *Int. J. Quantum Chem.* **2007**, 107, 311-317
33. Rulišek L., Šponer J., *J. Phys. Chem. B* **2003**, 107, 1913
34. Petrov A. S., Pack G.R., Lamm G., *J. Phys. Chem. B* **2004**, 108, 6072
35. Kabeláč M., Hobza P., *J. Phys. Chem. B* **2006**, 110, 14515-14523
36. Kosenkov D., Gorb L., Shishkin O., Sponer J., Leszczynski J., *Phys. Chem. B* **2008**, 112, 150

37. Gutlé C., Salpin J.-Y., Cartailier T., Tortajada J., Gaigeot M.-P., *J. Phys. Chem. A* **2006**, 110, 11684
38. Lamsabhi A.M., Alcamí M., Mó O., Yáñez M., Tortajada J., *J. Phys. Chem. A* **2006**, 110, 1943
39. Tsuchiya Y., Tamura T., Fujii M., Ito M., *J. Phys. Chem.* **1988**, 92, 1760-1765
40. Morsy M.A., Al-Somali A. M., Suwaiyan A., *J. Phys. Chem. B* **1999**, 103, 11205-11210
41. Hu X., Li H., Liang W., Han S., *J. Phys. Chem. B* **2005**, 109, 5935-5944
42. Hu X., Li H., Liang W., Han S. *J. Phys. Chem. B* **2004**, 108, 12999-13007
43. Kryachko E. S., Nguyen M. T., Zeegers-Huyskens T., *J. Phys. Chem. A* **2001**, 105, 1934-1943
44. Kryachko E. S., Nguyen M. T., Zeegers-Huyskens T., *J. Phys. Chem. A* **2001**, 105, 1288-1295
45. Wang N., Li P., Hu Y., Bu Y., Wang W., Xie X., *J. Theor. Comput. Chem.* **2007**, 6, 197-212
46. Fišer J., *Úvod do kvantové chemie*, 1. vydání, Academia **1983** (in Czech)
47. Polák R., Zahradník R., *Kvantová chemie - základy teorie a aplikace*, 1. vydání, SNTL **1985** (in Czech)
48. Nezbeda I., Kolafa J., Kotrla M., *Úvod do počítačových simulací - metody Monte Carlo a molekulární dynamiky*, 1. vydání, Karolinum **1998**
49. Shafternaar G., Noordik J.H., *J. Comput.-Aided Mol. Des.* **2000**, 14, 123
50. Gaussian 03, Revision A.1, M. J. Frisch, G. W. Trucks, H. B. Schlegel, G. E. Scuseria, M. A. Robb, J. R. Cheeseman, J. A. Montgomery, Jr., T. Vreven, K. N. Kudin, J. C. Burant, J. M. Millam, S. S. Iyengar, J. Tomasi, V. Barone, B. Mennucci, M. Cossi, G. Scalmani, N. Rega, G. A. Petersson, H. Nakatsuji, M. Hada, M. Ehara, K. Toyota, R. Fukuda, J. Hasegawa, M. Ishida, T. Nakajima, Y. Honda, O. Kitao, H. Nakai, M. Klene, X. Li, J. E. Knox, H. P. Hratchian, J. B. Cross, C. Adamo, J. Jaramillo, R. Gomperts, R. E. Stratmann, O. Yazyev, A. J. Austin, R. Cammi, C. Pomelli, J. W. Ochterski, P. Y. Ayala, K. Morokuma, G. A.

Voth, P. Salvador, J. J. Dannenberg, V. G. Zakrzewski, S. Dapprich, A. D. Daniels, M. C. Strain, O. Farkas, D. K. Malick, A. D. Rabuck, K. Raghavachari, J. B. Foresman, J. V. Ortiz, Q. Cui, A. G. Baboul, S. Clifford, J. Cioslowski, B. B. Stefanov, G. Liu, A. Liashenko, P. Piskorz, I. Komaromi, R. L. Martin, D. J. Fox, T. Keith, M. A. Al-Laham, C. Y. Peng, A. Nanayakkara, M. Challacombe, P. M. W. Gill, B. Johnson, W. Chen, M. W. Wong, C. Gonzalez, and J. A. Pople, Gaussian, Inc., Pittsburgh PA, **2003**.

51. Wu R., McMahon T. B., *J. Am. Chem. Soc.* **2007**, 129, 569
52. Kosenkov D., Gorb L., Shishkin O.V., Šponer J., Leszczynski J., *J. Phys. Chem. B* **2008**, 112, 150-157.
53. Gutlé C., Cartailier T., Tortajada J., Gageot M.P., *J. Phys. Chem. A* **2006**, 110, 11684-11694
54. Marino T., Mazzuca D., Toscano M., Russo N., Grand, A. *Int. J. Quantum Chem.* **2007**, 107, 311-317
55. Lamsabhi A.M., Mó O., Yáñez M., Boyd R.J., *J. Chem. Theory Comput.* **2008**, 4, 1002

## Appendices

*Table 17: Gas phase energies for uracil ... Mg<sup>2+</sup> complexes*

Structure	E <sub>comp</sub>	E <sub>Udef</sub>	E <sub>Uned</sub>	BSSE	E <sub>Def</sub>	E <sub>int</sub>	E <sub>rel-comp</sub>	E <sub>rel-taut</sub>
u13o2r_s4	-613.103638	-413.929619	-413.946491	2.03	10.59	-207.65	30.00	84.16
u13o2l_s4	-613.103117	-413.931117	-413.948643	2.05	11.00	-205.96	30.34	82.81
u13o4l_s2	-613.007540	-413.982101	-413.995485	1.24	8.40	-117.39	89.52	53.41
u13o4l_s5	-613.054829	-413.981841	-413.995485	1.28	8.56	-147.03	59.88	53.41
u13o4r_s1	-612.982513	-413.963295	-413.976213	1.22	8.11	-113.80	105.20	65.51
u13o4r_s4	-613.072270	-413.963163	-413.976213	1.68	8.19	-169.67	49.34	65.51
u1o2lo4l_s5	-613.039518	-413.951892	-413.964512	1.28	7.92	-156.86	69.49	72.85
u1o2lo4l_s6	-612.991790	-413.949964	-413.964512	1.53	9.13	-126.66	99.68	72.85
u1o2lo4r_s5	-613.048324	-413.932890	-413.942749	1.37	6.19	-175.96	64.05	86.50
u1o2lo4r_s6	-612.969580	-413.927774	-413.942749	1.40	9.40	-126.51	113.49	86.50
u1o2ro4l_s5	-613.053135	-413.965954	-413.978335	1.29	7.77	-156.72	60.95	64.17
u1o2ro4l_s6	-612.973183	-413.962117	-413.978335	1.12	10.18	-106.72	110.95	64.17
u1o2ro4r_s5	-613.064596	-413.948599	-413.958017	1.38	5.91	-176.57	53.85	76.92
u1o2ro4r_s6	-612.957997	-413.941204	-413.958017	1.11	10.55	-109.95	120.47	76.92
u3o2lo4l_s3	-613.019174	-413.968241	-413.983211	1.78	9.39	-131.86	82.75	61.11
u3o2lo4l_s5	-613.055829	-413.970106	-413.983211	1.27	8.22	-155.37	59.24	61.11
u3o2lo4r_s3	-612.971897	-413.944395	-c	1.61	-c	-c	-c	-c
u3o2lo4r_s4	-613.093696	-413.962193	-c	1.80	-c	-c	-c	-c
u3o2ro4l_s3	-613.025944	-413.955848	-413.969450	1.82	8.54	-144.71	78.54	69.75
u3o2ro4l_s5	-613.041766	-413.955982	-413.969450	1.27	8.45	-155.18	68.07	69.75
u3o2ro4r_s4	-613.083118	-413.949912	-c	1.80	-c	-c	-c	-c
u3o4r_s4	-613.045129	-414.016702	-414.063394	1.66	29.30	-97.95	66.35	10.80
uo2ro4r_s4	-613.041439	-414.022625	-414.065523	1.65	26.92	-94.31	68.65	9.46
u1_s3/s4	-613.113699	-414.064407	-414.080602	1.37	10.16	-130.47	23.03	0.00
u1_s1/s2	-613.098379	-414.063411	-414.080602	1.34	10.79	-120.89	32.61	0.00
u3o2l_s1	-613.081832	-414.034004	-414.052415	1.84	11.55	-127.69	43.49	17.69
u3o2l_s3	-613.089151	-414.034235	-414.052415	1.44	11.41	-132.69	38.50	17.69
u1o2r_s3	-613.106319	-414.047680	-414.064822	1.41	10.76	-135.70	27.70	9.90
u1o2r_s1	-613.043926	-414.050226	-414.064822	1.24	9.16	-96.72	66.68	9.90
u1o4l_s1	-613.146394	-414.031729	-414.047698	2.05	10.02	-170.96	3.19	20.65
u1o4r_s1	-613.139693	-414.025944	-414.042966	2.06	10.68	-169.71	7.41	23.62
u3o2l_s3	-613.140814	-414.038014	-414.052511	2.00	9.10	-164.48	6.64	17.63
u3o2l_s1	-612.979036	-414.031198	-414.052511	1.10	13.37	-63.86	107.26	17.63
u3o2r_s3	-613.143941	-414.022534	-414.036371	2.08	8.68	-176.50	4.76	27.76
u3o4l_s2	-613.151598	-414.037410	-414.052798	2.13	9.66	-170.95	0.00	17.45
u3o4l_s3	-613.111444	-414.039282	-414.052798	1.87	8.48	-146.01	24.94	17.45
u3o4r_s2	-613.142112	-414.047075	-414.063394	2.06	10.24	-158.40	5.89	10.80
u13o2lo4l_s1	-613.110561	-414.042864	-414.057374	1.82	9.11	-142.63	25.45	14.58
u13o2lo4l_s3	-613.081318	-414.041587	-414.057374	1.83	9.91	-124.27	43.80	14.58
u13o2lo4r_s1	-613.114744	-414.049071	-414.063743	1.84	9.21	-141.24	22.84	10.58
u13o2lo4r_s3	-613.009296	-414.042488	-414.063743	1.31	13.34	-75.60	88.48	10.58
u13o2ro4l_s2	-613.104364	-414.044122	-414.057503	1.83	8.40	-138.65	29.34	14.49
u13o2ro4l_3	-613.104363	-414.044134	-414.057503	1.83	8.39	-138.65	29.34	14.49
u13o2ro4l_6	-613.043974	-414.041353	-414.057503	1.22	10.13	-101.37	66.63	14.49
uo2ro4r_s2	-613.095620	-414.050074	-414.065523	1.85	9.69	-128.11	34.85	9.46

*Energies were calculated at MP2/6-311++G(2df,2pd)//B3LYP/6-311++G\*\* level of theory. See Table 12 for the description of the terms. See Figure 23 for the geometries of the structures.*